

Automatic Region Tracking of Brain Lesions in MRI Scans

MTHE 493 Thesis Report
Group 6

Authors: Katarina Camacho, 20069849

David Hoskin, 20053950

Kaitlyn Kobayashi, 20061712

David Lynch, 20058127

Nate Nethercott, 20071045

Supervisor: Professor Abdol-Reza Mansouri

Faulty of Engineering and Applied Science
Department of Mathematics and Engineering
Queen's University
Kingston, Ontario

April 10, 2021

Acknowledgements

The team would like to thank Dr. Abdol-Reza Mansouri for sharing his expertise, time, support and guidance throughout the course of the project.

The team would like to thank the Inter-university Consortium for Political and Social Research for allowing the team access and utilization of the data set used in designing and testing the solution produced.

The team would also like to acknowledge the principle investigator Sook-Lei Liew, USC Chan Division of Occupational Science and Occupational Therapy at the University of Southern California for all her hard work on compiling the data set.

Abstract

Accurate brain lesion segmentation for stroke patients is an important, time-consuming and tedious process. Several algorithms have been developed to tackle this problem, but manual lesion segmentation performed by a trained medical professional is still the gold standard in terms of accuracy. The objective of this project is to develop a region tracking algorithm that accurately segments off lesions given a sequence of MRI scans.

Region tracking algorithms are based on functionals encoded with information about the specific application space, including invariant properties between images in a sequence. Finding these invariant properties involves the analysis of the Anatomical Tracings of Lesions After Stroke (ATLAS) data set, a large ($n=304$) set of MRI scans performed on stroke victims with lesions manually segmented by trained medical professionals.

The invariant properties identified for use in the algorithm are the average intensity across the lesion region and the area covered by the lesion. The data set is reduced to lesions conforming closely to these invariants. The images are pre-processed to increase contrast and reduce noise.

To evaluate the effectiveness of the algorithm, it is compared to three other lesion segmentation algorithms. The metrics compared between the algorithms are the average computation time and the DICE similarity coefficient they achieve.

The social, ethical, environmental and economical impacts of general automated segmentation software and the developed automated segmentation algorithm are discussed in detail in the triple bottom line section. Ethical codes, standards and regulations are considered and taken into account. An economic analysis for the development, marketing, and sale of the algorithm is provided.

Table Of Contents

1	Introduction	1
1.1	General Introduction	1
1.2	Mathematical Problem Definition	1
1.3	MRI and Brain Lesion Background Information	2
1.4	Mathematical Background and Derivations	4
1.5	Existing Lesion Segmentation Algorithms	7
2	Problem	7
2.1	Problem Description	7
2.2	Problem Definition	7
2.3	Scope	7
2.4	Stakeholders	8
3	Problem Solution Goal	10
3.1	Solution Goal	10
3.2	Potential Applications	10
4	Design Process	10
4.1	Design Process Overview	10
4.2	Data Set Analysis	11
4.3	Data Set Changes	11
4.4	Metrics for Algorithm Analysis	13
4.5	Design Iterations	13
4.5.1	Area Invariance based Design	13
4.5.2	Average Intensity Invariance based Design	17
4.5.3	Image Pre-Processing	22
5	Design Solution	27
5.1	General Solution Description	27
5.2	Assumptions and Approximations	27
5.3	Functional	28
5.4	Results	28
5.5	Solution Limitations	31
6	Implementation Evaluation	32
6.1	Solution Evaluation	32
6.1.1	Total Average Runtime	32
6.1.2	Average Dice Similarity Coefficient	32
6.2	Compared to Existing Solutions	33
6.2.1	Manual Segmentation	33
6.2.2	Existing Auto-Segmentation Algorithms	33
7	Triple Bottom Line Impacts, Ethics, and Economic Analysis	34
7.1	Social Impacts and Considerations	34
7.2	Standards, Codes, and Ethical Considerations	35
7.3	Environmental Impacts and Considerations	35
7.4	Economic Impacts and Considerations	36

7.5	Economic Analysis	36
8	Next Steps	37
9	Conclusion	38
References		56

List of Figures

1	Image displaying the region of interest in region tracking, and how the image is interpreted in the image domain	1
2	Sequence of layers in an individual MRI scan of a human brain [5]	2
3	T1 weighted MRI image with gadolinium injection displaying metastatic brain lesions [7]	3
4	Brain lesion MRI scans from patients with various medical conditions [9].	4
5	Lesion with >100% change in area between slices	11
6	Sample lesion from reduced data set	12
7	Algorithm output using area functional	14
8	Dice score vs layer for area functional design	15
9	Algorithm output using area and arc length functionals	16
10	Dice score vs layer for area and arc length functionals design	17
11	Algorithm output using intensity and arc length functionals	18
12	Dice score vs layer for intensity and arc length functionals design	19
13	First image in a sequence using intensity functional	20
14	Second image in a sequence using intensity functional	21
15	Third image in a sequence using intensity functional	22
16	Intensity histogram of image prior to histogram equalization	23
17	Intensity histogram of image after histogram equalization	24
18	MRI image prior to histogram equalization (left) and post histogram equalization (right)	25
19	Image segment before pre-processing	26
20	Image segment after pre-processing	26
21	Finalized algorithm performance on benchmark scans	29
22	Finalized algorithm performance on benchmark scans, no image processing	30
23	Finalized algorithm performance on benchmark scans, supervision for 2 stages	31
24	Metastasis with clear border and regular image intensity	37

List of Tables

1	Stakeholders accounted for when designing automated region tracking algorithm for tracing brain lesions in stroke patients.	9
2	Intensity observations on reduced data set	12
3	Intensity observations, ctd.	12
4	Area observations on reduced data set	12
5	Center of mass observations for reduced data set	13
6	File legend for Table 7	32
7	DSC values per slice	33
8	Average DSCs	33

9	Comparison of region tracking algorithm to existing software	34
---	--------------------------------------------------------------	----

1 Introduction

1.1 General Introduction

Given a sequence of images, region-tracking is the problem of identifying a region of an image that is of interest and identifying this region in the other images in the sequence. For this problem, images are represented as functions mapping from some image domain to an output space. The input could be an individual pixel on a screen and the output could be a real number indicating brightness or a point in R^3 indicating an RGB value.

Consider Figure 1. Suppose the pear and the books are a region of interest in the image. The region of interest can be interpreted as a shadow on the image domain. The problem of region tracking becomes identifying the shadow on the image domain that maps to the region of interest in the next image in the sequence.

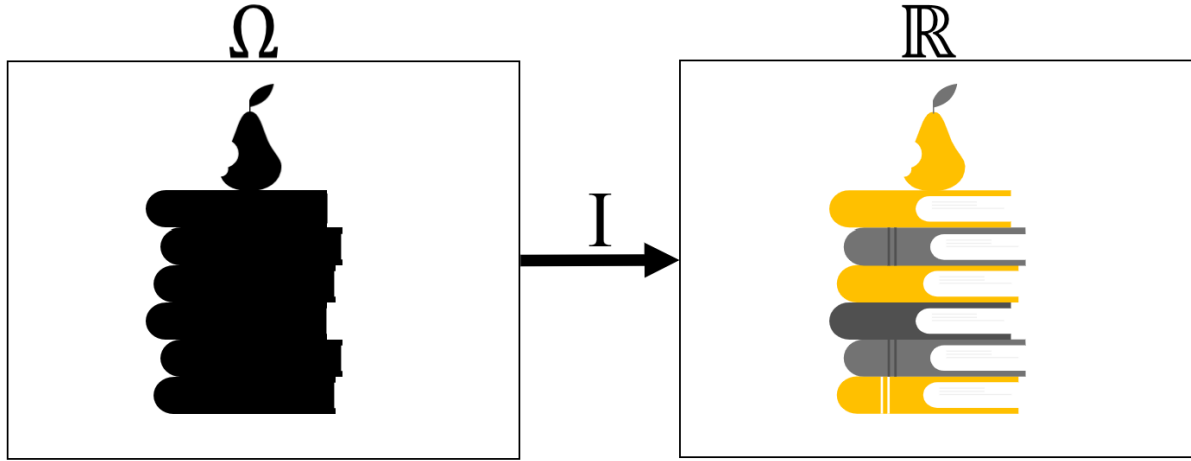


Figure 1: Image displaying the region of interest in region tracking, and how the image is interpreted in the image domain

1.2 Mathematical Problem Definition

The problem of region-tracking can be defined mathematically as follows. Let Ω be the image domain. Two images are defined as $I_0, I_1 : \Omega \rightarrow R$. Let $R_0 \subset \Omega$ be the subset of the image domain that defines the region of interest. Let \mathcal{C} be a collection of subsets of the power set of Ω . \mathcal{C} is known as the candidate set and it corresponds to the set of possible subsets of Ω that could potentially be the region of interest. Define $E_{(R_0, I_0, I_1)} : \mathcal{C} \rightarrow R$ and let $R_1 \subset \Omega$ be the unique minimizer of $E_{(R_0, I_0, I_1)}$ [1].

The problem of tracking a region through a sequence of images is defining an appropriate functional, E , such that R_1 is the region of interest for the next image in the sequence. The definition of the functional depends on the specific problem application space. When designing a functional, it is useful to understand what properties of the region are invariant between images in the sequence. These invariant properties can be encoded into the functional so that the unique minimizer is the desired region of interest.

Once the invariant properties of the region have been studied and an appropriate functional defined, the problem becomes developing a method to reach the unique minimizer.

1.3 MRI and Brain Lesion Background Information

Magnetic resonance imaging (MRI) is a frequently used medical scanning technology. MRI is the most commonly used imaging test for the brain and spinal cord [2]. In particular, an MRI scan is useful for diagnosing tumors, strokes, and other brain injuries [2].

An MRI scanner generates a strong magnetic field that aligns the axes of the hydrogen protons within the body of the patient [3]. The strength of the magnetic field produced is altered locally to generate images of slices of the patient's body [3]. A series of scans are produced where each show a layer of the patient's body or brain, as seen in Figure 2. Modern MRI scanners can also generate sequences that are focused on specific types of tissue [4]. This can be useful for doctors when considering a specific diagnosis or disease.

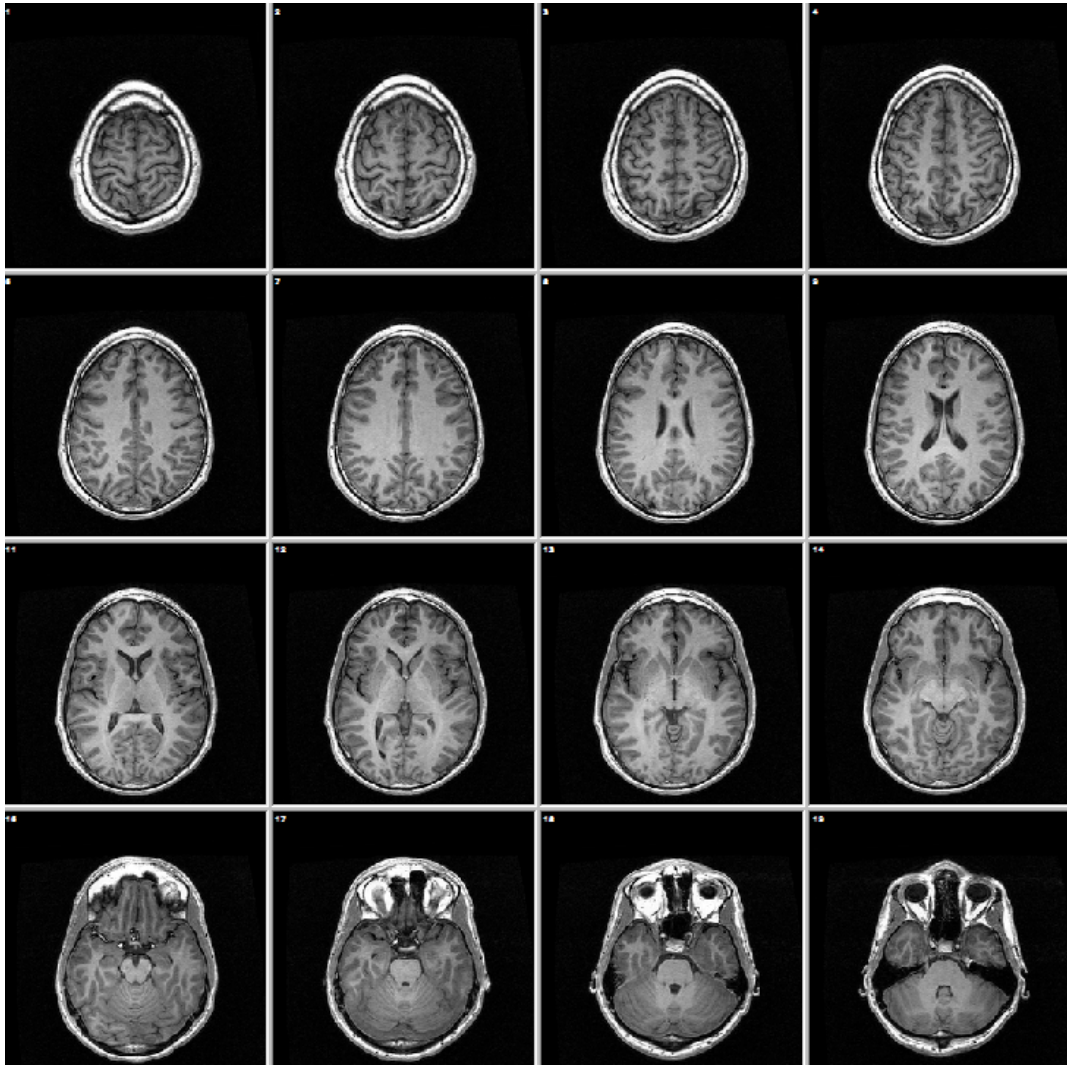


Figure 2: Sequence of layers in an individual MRI scan of a human brain [5]

In particular, brain lesions, which are damaged tissues in the brain, can be diagnosed through MRIs. Brain lesions may cause edema (i.e. swelling) in the brain, which can give the patient headaches or loss of brain function [6]. This can lead to the doctor requesting an MRI. There are two types of MRIs: T2 weighted sequences and T1 weighted sequences.

T2 weighted sequences are used when the doctor expects the patient to have swelling in their brain [6]. In T2 weighted MRI sequences swelling (i.e. the more watery substances) appear bright/white, causing brain lesions to appear bright/white [6].

In T1 weighted MRI sequences, water appears dark, and thus lesions appear dark. However, if the radiologist suspects the patient to have brain lesions, they will inject them with gadolinium. Since lesions break the blood-brain barrier, this causes the gadolinium to seep out into the lesion, resulting in the lesions appearing bright/white [6]. This can be seen in the figure below, Figure 3.

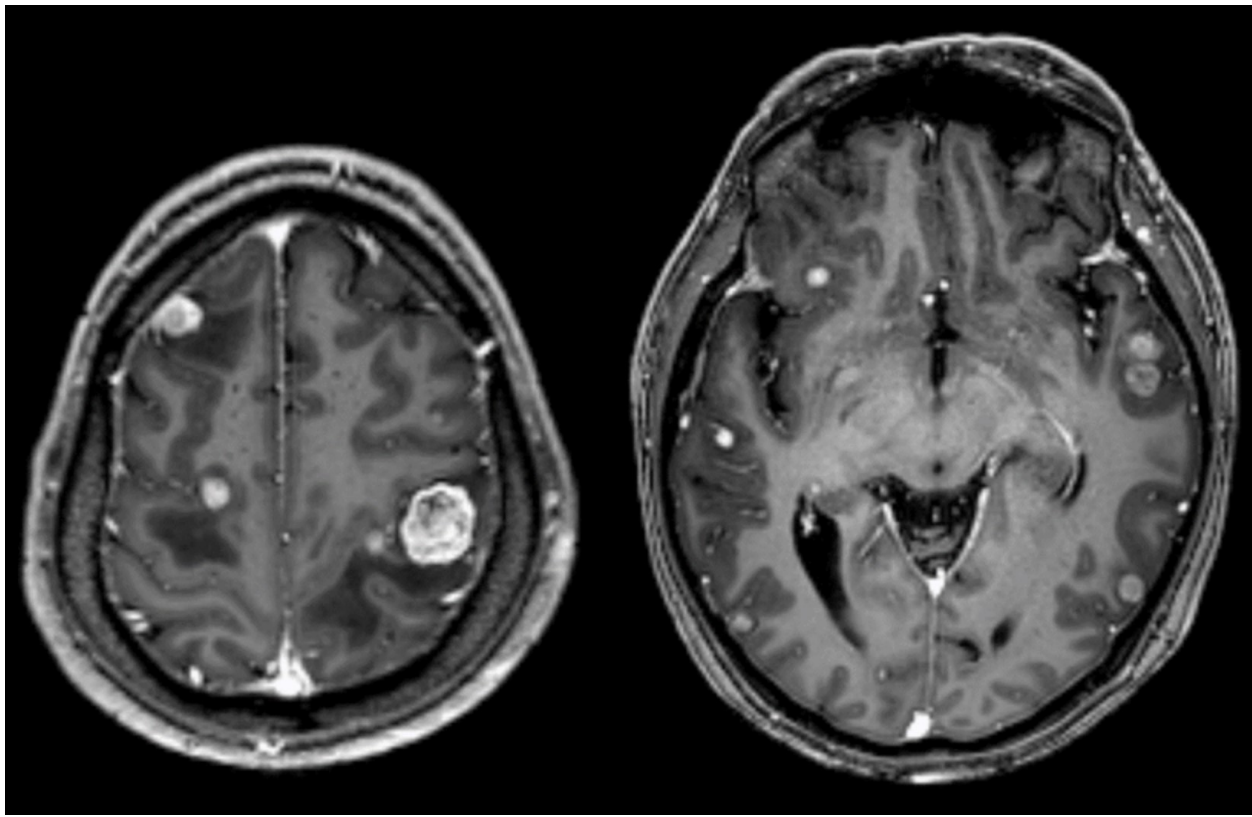


Figure 3: T1 weighted MRI image with gadolinium injection displaying metastatic brain lesions [7]

There are many different types of brain lesions, which can be due to tumors, strokes, multiple sclerosis, aneurysms, epilepsy, etc. [8]. Although they may appear different in MRIs, in general they appear bright. Some brain lesions are typically much easier to identify, such as metastases. Metastatic brain lesions are tumors, which have spread from other parts of the body. In MRIs, these often are well-defined (i.e. have a clear edge) and are bright [6]. They are also often found near the cerebellum, making them much easier to locate and identify [6]. However, there exists lesions that may not be as well-defined and may not have clear edges. Some lesions may cause edema (i.e. swelling), and break, causing non-lesion areas of the MRI scan to appear bright [6]. These cases are

less common, and thus will not be the focus of the problem. Overall, the majority of lesions are well-defined and a different intensity than the surrounding tissue. This is an assumption which was carried throughout the project.

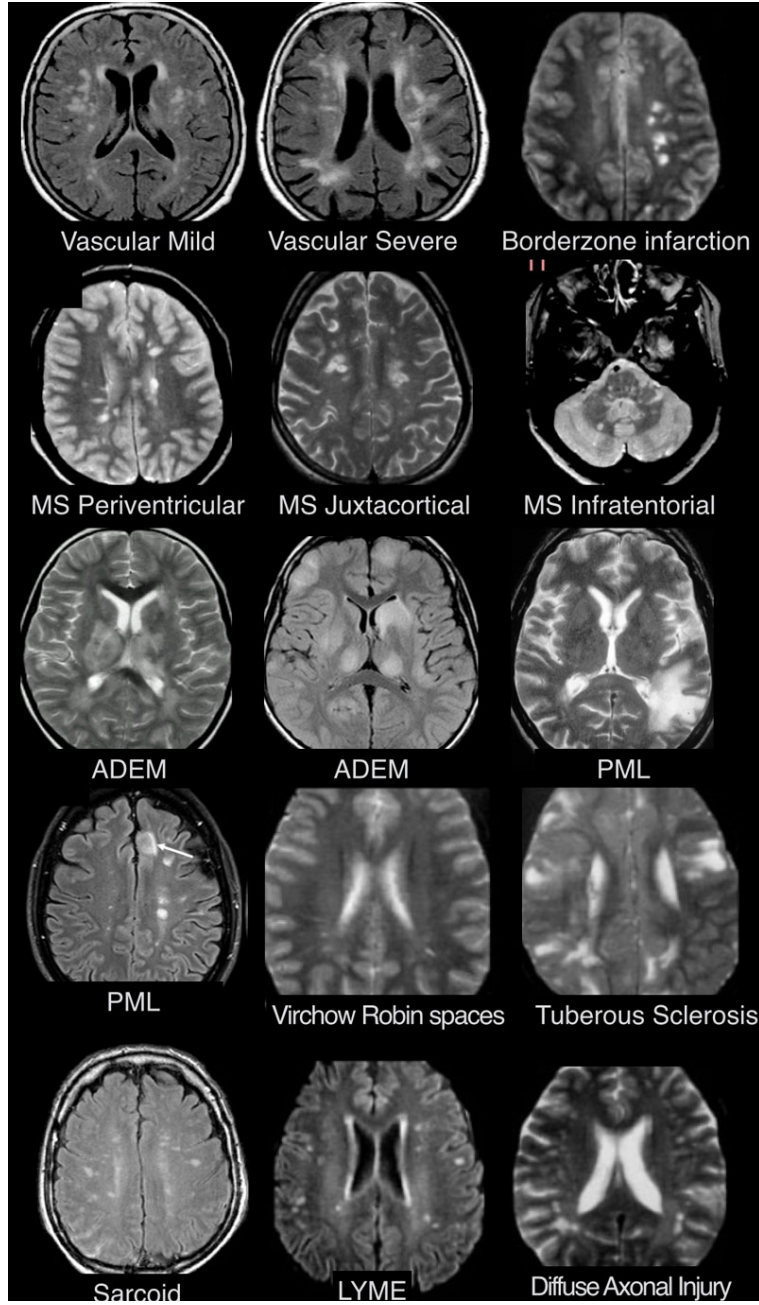


Figure 4: Brain lesion MRI scans from patients with various medical conditions [9].

1.4 Mathematical Background and Derivations

The region of interest can be represented in two main ways, explicitly or implicitly. For the explicit representation, the boundary of the region is defined as a curve. This method assumes that the boundary of the region is smooth and requires that the curve is closed [10]. Mathematically, this

representation can be seen in Equation 1. The implicit representation is known as the level set representation. The region of interest is defined as the boundary between the positive and negative outputs of the defined implicit representation function [10]. Mathematically, this representation can be seen in Equation 2.

$$\begin{aligned}\vec{\gamma} : [0, 1] &\rightarrow \mathbb{R}^2 \\ s &\mapsto \vec{\gamma}(s)\end{aligned}\tag{1}$$

$$\begin{aligned}\text{Let } u : \mathbb{R}^2 &\rightarrow \mathbb{R} \text{ such that:} \\ \{(x, y) \in \mathbb{R}^2 | u(x, y) = 0\} &= \{\vec{\gamma}(s) | s \in [0, 1]\}\end{aligned}\tag{2}$$

Given a representation of the region and a functional, the problem becomes evolving the solution over time so that it converges to the unique minimizer. Gradient descent is such a method to algorithmically reach the minimizer. Given a functional, the Gradient Descent PDE for a curve is given by Equation 3 [10]. For the level set method, the corresponding Level Set PDE is given by Equation 4 [10].

$$\frac{\partial \vec{\gamma}}{\partial t} = \frac{-\partial E}{\partial \vec{\gamma}} \approx F \hat{N}\tag{3}$$

$$\frac{\partial u}{\partial t} = -F \|\vec{\nabla} u\| \tag{4}$$

Seen below in Equation 5 is the functional designed to penalize arc length [10]. This functional tends to cause the the unique minimizer to be a simpler and smoother curve. The Gradient Descent and Level Set PDEs can be seen in Equation 6 and Equation 7 respectively. λ is a regularization parameter, κ is the curvature, and \hat{N} is the unit normal.

$$E(\vec{\gamma}) = \lambda \oint_{\vec{\gamma}} ds \tag{5}$$

$$\frac{\partial \vec{\gamma}}{\partial t} = -\lambda \kappa \hat{N} \tag{6}$$

$$\frac{\partial u}{\partial t} = \lambda \kappa \|\vec{\nabla} u\| \tag{7}$$

Seen below in Equation 8 is the functional designed to have the region converge to one with a certain area, A_0 . The derivation of the Gradient Descent and Level Set PDEs follow with results seen in Equation 9 and Equation 10 respectively.

$$E(\vec{\gamma}) = \left(\iint_{R_{\vec{\gamma}}} dx dy - A_0 \right)^2 \tag{8}$$

$$\begin{aligned}
\frac{\partial \vec{\gamma}}{\partial t} &= \frac{-\partial E}{\partial \vec{\gamma}} \\
\frac{\partial \vec{\gamma}}{\partial t} &= 2 \left(\iint_{R_{\vec{\gamma}}} dx dy - A_0 \right) \frac{\partial}{\partial \vec{\gamma}} \left(\iint_{R_{\vec{\gamma}}} dx dy - A_0 \right) \\
\frac{\partial \vec{\gamma}}{\partial t} &= 2 \left(\iint_{R_{\vec{\gamma}}} dx dy - A_0 \right) \hat{N}
\end{aligned} \tag{9}$$

$$\frac{\partial u}{\partial t} = - \left[2 \left(\iint_{R_{\vec{\gamma}}} dx dy - A_0 \right) \right] \|\vec{\nabla} u\| \tag{10}$$

Seen below in Equation 11 is the functional designed to preserve the average intensity within the region between images in the sequence [10]. The derivation of the Gradient Descent and Level Set PDEs follow with results seen in Equation 12 and Equation 13 respectively.

$$E(\vec{\gamma}) = (\mu_{I_1}(R_{\vec{\gamma}}) - \mu_{I_0}(R_0))^2 \tag{11}$$

$$\text{with } \mu_I(R) = \frac{\int_R I(x, y) dx dy}{\int_R dx dy}$$

$$\begin{aligned}
\frac{\partial \vec{\gamma}}{\partial t} &= \frac{-\partial E}{\partial \vec{\gamma}} \\
\frac{\partial \vec{\gamma}}{\partial t} &= -2 (\mu_{I_1}(R_{\vec{\gamma}}) - \mu_{I_0}(R_0)) \frac{\partial}{\partial \vec{\gamma}} (\mu_{I_1}(R_{\vec{\gamma}})) \\
\frac{\partial \vec{\gamma}}{\partial t} &= -2 (\mu_{I_1}(R_{\vec{\gamma}}) - \mu_{I_0}(R_0)) \frac{\left(\int_{R_{\vec{\gamma}}} dx dy \right) \frac{\partial}{\partial \vec{\gamma}} \left(\int_{R_{\vec{\gamma}}} I_1 dx dy \right) - \left(\int_{R_{\vec{\gamma}}} I_1 dx dy \right) \frac{\partial}{\partial \vec{\gamma}} \left(\int_{R_{\vec{\gamma}}} dx dy \right)}{\left(\int_{R_{\vec{\gamma}}} dx dy \right)^2} \\
\frac{\partial \vec{\gamma}}{\partial t} &= -2 (\mu_{I_1}(R_{\vec{\gamma}}) - \mu_{I_0}(R_0)) \frac{\left(\int_{R_{\vec{\gamma}}} \vec{\gamma} dx dy \right) I_1 - \left(\int_{R_{\vec{\gamma}}} \vec{\gamma} I_1 dx dy \right)}{\left(\int_{R_{\vec{\gamma}}} dx dy \right)^2} \hat{N}
\end{aligned} \tag{12}$$

$$\frac{\partial u}{\partial t} = 2 (\mu_{I_1}(R_{\vec{\gamma}}) - \mu_{I_0}(R_0)) \frac{\left(\int_{R_{\vec{\gamma}}} \vec{\gamma} dx dy \right) I_1 - \left(\int_{R_{\vec{\gamma}}} \vec{\gamma} I_1 dx dy \right)}{\left(\int_{R_{\vec{\gamma}}} dx dy \right)^2} \|\vec{\nabla} u\| \tag{13}$$

The evolution equations discussed so far have all been continuous. For these equations to be implemented in a computational setting they need to be appropriately discretized. One such approach is Euler's Method [11]. A time step is defined as Δt and the mathematical expression for this process can be seen in Equation 14 for the general Gradient Descent PDE and in Equation 15 for the general Level Set PDE.

$$\vec{\gamma}_{i+1} = \vec{\gamma}_i - \Delta t \frac{\partial E}{\partial \vec{\gamma}}(\vec{\gamma}_i) \tag{14}$$

$$u_{i+1} = u_i - \Delta t F \left\| \vec{\nabla} u_i \right\| \quad (15)$$

1.5 Existing Lesion Segmentation Algorithms

Given that manual tracing of lesions is a time-consuming and labor-intensive process, several algorithms have been developed to try and solve the problem of automating lesion segmenting. For the purposes of this project, three other publicly available segmentation algorithms that have been developed in the past 10 years will be considered: Automated Lesion Identification (ALI), Gaussian naive Bayes lesion detection (lesionGnb), and lesion identification with neighborhood data analysis (LINDA).

ALI's primary algorithm is the support-vector machine supervised learning model, lesionGnb's primary algorithm is the Gaussian naive Bayes classification algorithm, and LINDA's main algorithm is the random decision forest algorithm. Of the three algorithms, LINDA performs the best in terms of accuracy, but is the most computationally expensive.

In a 2019 study by Ito et al., these three algorithms were been tested extensively on T1-weighted MRI scans of chronic stroke lesions [12], the same type of scans that this project operates on. The results from this paper will be used in the evaluation of the project's performance.

2 Problem

2.1 Problem Description

As noted in Section 1.3, brain lesions can be a result of a number of diseases, and can have different appearances in MRI scans. Despite this, strokes, vascular injury and impaired blood supply to the brain are the leading causes of brain lesions [8]. Although they appear bright/white in T2 weighted MRI sequences and T1 weighted MRI sequences with a gadolinium injection, the brain lesions must not be mistaken for brain folds, the skull, or other fluids in the brain due to breakage of the lesion. Some lesions are generally easier to identify than others, as some are well-defined (i.e. have a clear edge) and are very bright/white. Complex and large lesions can take doctors several hours to trace through the various MRI images [13], which can be extremely inefficient, especially when treatment is required as quickly as possible to reduce the likelihood and severity of long-term disabilities. Additionally, it is crucial to identify all lesions in all scans to understand their depth in the brain, as lesions in particular areas of the brain can have certain side effects on the patient, and may require immediate surgery. It is also extremely important for doctors to identify the patient's brain lesions early on, allowing them to monitor if the lesions are healing.

2.2 Problem Definition

Identifying and tracing stroke related brain lesions in a sequence of MRI images, is a time-consuming and tedious process. Thus, medical practitioners require a reliable, accurate, and efficient tool to track brain lesions throughout a sequence of brain scans to identify the areas of the brain affected.

2.3 Scope

The application providing the solution to this problem limits its scope to well-defined, solid and high-contrast lesions in stroke patients. The lesions should have a relatively consistent shape from slice to slice. This can be somewhat controlled by the spacing between slices attribute, when taking

an MRI scan. Only high contrast MRI scans should be used. Additionally, the solution is not meant to completely eliminate the need for radiologists to trace through scans, but instead is meant to be used as an assistive tool.

2.4 Stakeholders

When designing and implementing the solution to this problem, the needs and impact on radiologists, patients and existing lesion tracing technology companies were taken into consideration. These were the main three stakeholders, however, there were additional stakeholders, which can be found in Table 1.

Radiologists require the solution to be accurate and reliable, as it must accurately and reliably locate the lesion in each image. The solution should also trace the lesions faster than tracing by hand, and should not be extremely expensive. This includes the purchase of the software, the running of the software, and any additional hardware it must be ran on. In general, things radiology departments consider prior to purchasing medical software technology includes performance, integration, implementation, finances, quality and safety [14]. Additional beneficial features to radiologists include a measuring feature to determine the lesion's size and distance from the skull, as well as a feature that can compare the scans to previous scans to determine if lesions have healed/are healing.

Patients require the software to accurately identify the general region of the brain impacted by the lesion to identify any potential affects this could have on them. Additionally, the system must be somewhat fast, to shorten the patient's wait-time on their results.

Existing lesion tracing technology companies may require this solution to be more accurate, efficient, reliable, and/or adaptable than their pre-existing solution(s), if they wish to purchase the solution.

Table 1: Stakeholders accounted for when designing automated region tracking algorithm for tracing brain lesions in stroke patients.

Stakeholder	Economic	Social	Environmental
Radiologist	The solution must allow them to more effectively use their time, allowing them to help more patients. In countries with privatized healthcare, this could result in the radiology clinics making more money.	Utilizing the solution adds an extra layer of protection, helping the doctors ensure they have identified all lesions.	The solution should not use an extraneous amount of electricity and computer power.
Patient	In countries with privatized healthcare, this could help make this process a little bit more affordable to the patients.	The solution should be accurate and reliable, to help the patient understand the regions of their brain affected by the lesion, and the impact this has on them. Additionally, if the solution reduces their wait-time on their results, this allows the patient to receive any necessary procedure to follow, a little faster.	
Existing Lesion Tracing Technology Companies	The solution must be reasonably priced for them to purchase ownership. The solution must be projected to earn them enough money to at least break even.	The solution should not have any ethical concerns, which would damage the company's reputation.	The solution must not be environmentally polluting, and should be somewhat more energy efficient than existing solutions.
Hospitals	The solution must not be too expensive for the hospitals to pay for.	The solution must not have any ethical concerns.	The solution should not require an extensive amount of energy.
Government	The solution should allow radiologists to more effectively use their time and help patients, as the government funds healthcare in Canada.		
Insurance	Insurance companies that insure doctors could potentially save money if the application helps prevent lawsuits.		
General population		There should not be any ethical concerns by facilities using this software.	If the software solution requires additional hardware, the manufacturing of this technology may require metals that need to be mined. This involves removing resources that are sometimes scarce from the earth, which could release harmful chemicals and pollutants into the air, ground and water.

3 Problem Solution Goal

3.1 Solution Goal

The team's solution goal to this problem is to implement an application which traces the border of a brain lesion, given a sequence of MRI scans and an initial scan with the lesion traced by a doctor. The solution will utilize various mathematical tools, including the calculus of variations, partial differential equations, the level set method, and functionals. Thus, the radiologist should be able to upload the MRI scans, then trace the lesion in only one scan, and then the software should return all subsequent scans with the lesion traced. This software is not meant to completely eliminate the need for radiologists to trace through scans, but instead is meant to be used as an assistive tool for the radiologist to use to speed up their lesion tracing process, and double check to make sure they didn't miss something important.

3.2 Potential Applications

Although the solution proposed is meant to be used on stroke patients, it could be easily adapted to other applications. Since metastatic brain lesions are clearly visible, they will be able to be detected by the software much more easily. By simply adding to the code in the software, a function to measure the metastatic lesion's distance from the skull can be implemented. This would be extremely useful to doctors when radiation is required to remove the metastases. Additionally, by calculating the area of the lesion in each scan, the software can help doctors determine whether the radiation is working, causing the metastases to shrink overtime. Another potential application, is to assist doctors in monitoring a patient's multiple sclerosis (MS). As older lesions heal, they create holes in the patient's brain, which are not enhanced in the MRI scans. Thus, using the software on MS patients could help doctors identify whether older lesions have healed and disappeared.

4 Design Process

4.1 Design Process Overview

When approaching the problem, the team followed the engineering design process, which included identifying and defining the problem, gathering information, identifying potential solutions, creating a prototype, evaluating and testing the prototype, then continuing to refine and retest/evaluate the solution until the final solution was obtained.

The team began the project by defining and redefining the problem at hand, narrowing the scope, and identifying all relevant stakeholders.

When gathering information, the team researched manual lesion tracing, existing lesion tracing algorithms, and potential solution evaluation methods. Information was gathered through doing an initial search on the internet regarding the problem, reading scholarly journal articles and patents, and interviewing a radiologist. While continuing to research, the team learned about useful mathematical background information, which would assist in designing the solution. This information was learned through meetings with Dr. Abdol-Reza Mansouri, as well as reading related mathematical published papers and books. The team also obtained a data set containing MRIs of stroke patients with brain lesions, and analyzed this data set to identify consistencies in the images of the lesions, and identify any abnormalities in the data set.

Through research and analysis of the data set, the team created potential functionals for potential solutions. These functionals were implemented, and combined and tested to eventually allow the team to reach the final solution. The team also tested image filtering to help denoise the images, and pre-process them prior to the lesion tracing.

4.2 Data Set Analysis

All testing was performed on the Anatomical Tracings of Lesions After Stroke data set, with permission from the Inter-university Consortium for Political and Social Research (ICPSR). The data set is comprised of 304 T1-weighted MRI scans of chronic stroke lesions, and each scan includes a binary mask detailing each pixel that is part of the lesion.

To develop region tracking functionals, the team began looking for metrics that were shared between all of the lesions. The following metrics were observed: Area covered by the lesion, the center of mass of the lesion, and the image intensity within the lesion. The MRIs were put through a first order differential filter in order to observe the change in intensity in the X and Y directions. For each of these metrics, the average on each slide, the average over all slides, the change, the average change between all slides, the variance from the average, and more were recorded. Note that some of the intensity values were very large and some were very small; this is because not all of the scans share the same image intensity range.

4.3 Data Set Changes

The invariants the solution algorithm was based on were the average change in area and the average intensity over the lesion region. While reviewing our algorithm's performance on different lesions, it was found that many of the lesions caused the algorithm to misbehave, since they did not share the invariant properties possessed by most of the lesions in the data set. For instance, some lesions experienced massive changes in the area they covered between MRI slices, as seen below in Figure 5.

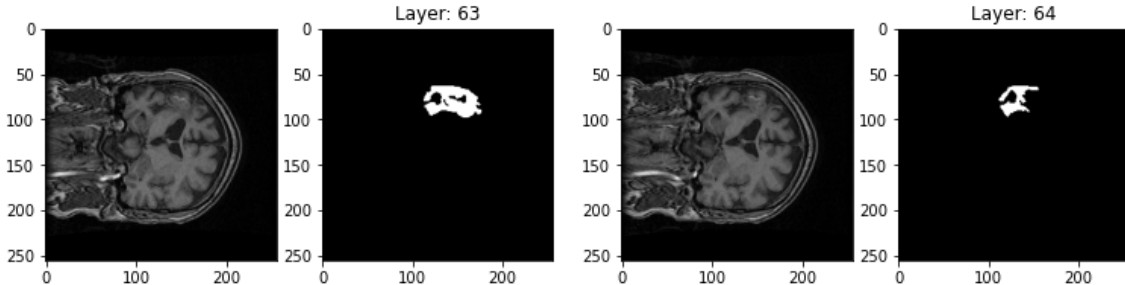


Figure 5: Lesion with $>100\%$ change in area between slices

These scans were then removed from the data set, as it was outside the scope of the problem. For steps detailing how to solve this problem, please see Section 8. The resulting data set was then comprised of simply shaped lesions consistent with the invariant measures. For full results, see the Appendix (Section).

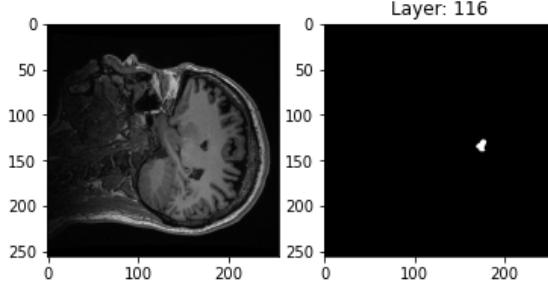


Figure 6: Sample lesion from reduced data set

Table 2: Intensity observations on reduced data set

	file	Max Intensity	Min Int.	Average Int.	Max Δ Int.	Min Δ Int.
0	c0001s0005t01.nii.gz	66.55056	58.46479	62.01592	4.837728	0.15401
1	c0002s0002t01.nii.gz	72.1	59.84146	64.03593	4.637037	0.102346
2	c0002s0005t01.nii.gz	70.9372	51.27586	65.09498	8.213511	0.002439
3	c0002s0020t01.nii.gz	48.3	30.86441	40.79082	8.789844	1.769992
4	c0003s0014t01.nii.gz	2488.2	1323.917	1730.583	412.6878	39.31487
5	c0003s0020t01.nii.gz	2635.045	1796.655	2057.221	312.4865	7.899895
6	c0003s0037t01.nii.gz	1014.732	560.3333	840.5234	225.4591	19.76806
7	c0004s0034t01.nii.gz	2554.5	1195.822	1812.442	483.0172	4.064103
8	c0005s0012t01.nii.gz	140.4091	96.88	118.7749	21.125	0.486522
9	c0005s0045t01.nii.gz	392.1667	231.0841	281.0512	96.38889	9.34076

Table 3: Intensity observations, ctd.

	Average ΔInt.	Max Variance	Min Variance	Average Variance	Max Δ Var.	Min Δ Var.	Average Δ Var.
0	1.438558	187.3192	4.320988	72.52349	44.38861	0.989436	14.63063
1	1.05084	66.16102	3.29	42.26579	27.58052	1.767055	8.855897
2	2.663852	257.6285	17.20889	91.31472	156.5204	1.244872	34.53307
3	5.853569	210.4513	50.11721	129.5144	108.6006	4.921104	63.97919
4	175.7367	584560.2	26797.96	341603.2	322611.2	27589.04	133791.8
5	110.7469	485977.9	702.25	261304.5	241085.4	4760.579	76239.68
6	83.15042	149541.5	12045.06	103081.9	84224.35	6469.245	23454.57
7	132.3815	711987.9	25863.19	437432.6	288550.7	1704.596	87837.65
8	8.654829	2889.811	42.25	1983.18	1806.109	1.489136	432.9172
9	32.54052	7682.089	1379.139	4511.058	3276.812	325.9699	1491.914

Table 4: Area observations on reduced data set

	file	Average Area	Average Δ Area	Max Area	Max Δ Area	Min Area	Min Δ Area
0	c0001s0005t01.nii.gz	238.1364	29.2093	432	105	9	1
1	c0002s0002t01.nii.gz	172.4583	30.34783	352	240	4	2
2	c0002s0005t01.nii.gz	132.5556	31.65385	217	89	34	1
3	c0002s0020t01.nii.gz	64.33333	29.875	103	57	21	3
4	c0003s0014t01.nii.gz	65.36364	19.9	106	42	3	4
5	c0003s0020t01.nii.gz	90.77778	17.05882	157	58	2	1
6	c0003s0037t01.nii.gz	83.9	22.33333	119	46	12	2
7	c0004s0034t01.nii.gz	84.65217	16.59091	186	60	4	1
8	c0005s0012t01.nii.gz	96.4	25.85714	191	54	2	1
9	c0005s0045t01.nii.gz	64.7	21.22222	107	69	6	1

Table 5: Center of mass observations for reduced data set

	file	Average X	Average Y	Max Distance	Min Distance	Average Distance
0	c0001s0005t01.nii.gz	103.8343884	150.3587508	3.694564692	0.169538526	1.378148792
1	c0002s0002t01.nii.gz	154.8053918	139.3450638	11.17554459	0.142568826	1.53370924
2	c0002s0005t01.nii.gz	159.3924474	153.6351624	7.026728003	0.366936322	2.057911863
3	c0002s0020t01.nii.gz	99.68425604	132.8839892	4.635125524	0.508380414	2.31155455
4	c0003s0014t01.nii.gz	133.4402982	171.2100964	3.721674918	0.641480923	1.846537996
5	c0003s0020t01.nii.gz	123.8523061	171.8797992	1.025501288	0.163888694	0.587745306
6	c0003s0037t01.nii.gz	111.6564127	171.1875299	4.750982278	0.642780516	2.56266841
7	c0004s0034t01.nii.gz	51.86730322	81.43517605	3.623150416	0.397510562	1.133369969
8	c0005s0012t01.nii.gz	155.0691686	58.46838782	4.235540128	0.589623821	2.455294023
9	c0005s0045t01.nii.gz	123.1395814	88.30947945	0.886764437	0.184934647	0.50278135

4.4 Metrics for Algorithm Analysis

There were two metrics chosen to evaluate the algorithms created throughout the design process. These were average computational time and average Dice Similarity Coefficient (DSC) [15]. The former was chosen to measure how time-efficient the algorithm would be compared to manual segmentation and other auto-segmentation algorithms, while the latter was chosen to measure accuracy.

Average computational time per slice was defined to be the average amount of time it took an algorithm to generate one segmentation on an MRI lesion slice. From there, the total average computational time was calculated by taking the average computational time per slice, multiplying it by the average number of slices for a lesion, and then adding 120 s to simulate the amount of time needed for a specialist to segment the first image.

The DSC is a commonly used metric for evaluating segmentation algorithms in medical imaging. In its most basic form, the DSC is an equation which measures the similarity between two sets. The equation for the DSC is seen in Equation 16 below.

$$DSC = \frac{2|X \cap Y|}{|X| + |Y|} \quad (16)$$

For the purposes of this application, the set X represents the set of all pixels corresponding to the manual segmentation and its interior and the set Y represents the set of all pixels corresponding to the algorithm's segmentation and its interior. The DSC equation will yield a number between 0 and 1, with 1 representing an exact overlap between the two segmentations and 0 representing the sets being disjoint from one another. With manual segmentation being taken as the ground truth, the results of the DSC will give a good representation of how well the algorithm can segment the lesion itself.

4.5 Design Iterations

4.5.1 Area Invariance based Design

The file labelled c0002s0004t01 was used as the test file for the trials for the various design iterations so that comparisons between the different designs could be made.

From the data exploration conducted earlier in the design process, it was found that the area of the lesions tended to change only a small amount from layer to layer. This information was used and the functional seen in Equation 8 was used to encode this information in the algorithm. Testing the algorithm using only this functional with the test file yielded the result in Figure 7. The plot of dice scores by layer can be seen in Figure 8. The average dice score for this trial was 0.428. The algorithm was reasonably effective in tracing the lesion through the first 4 to 5 layers, but after this point the contour created by the algorithm tended to become increasingly complex and convoluted. This indicated that the arc length would need to be penalized in future iterations of the design to remove this behaviour.

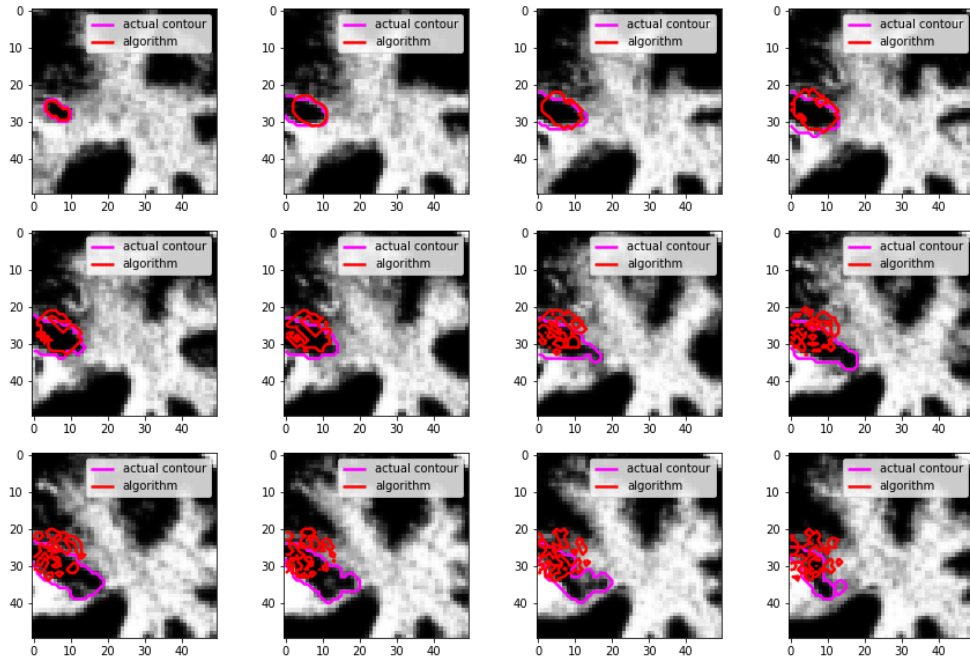


Figure 7: Algorithm output using area functional

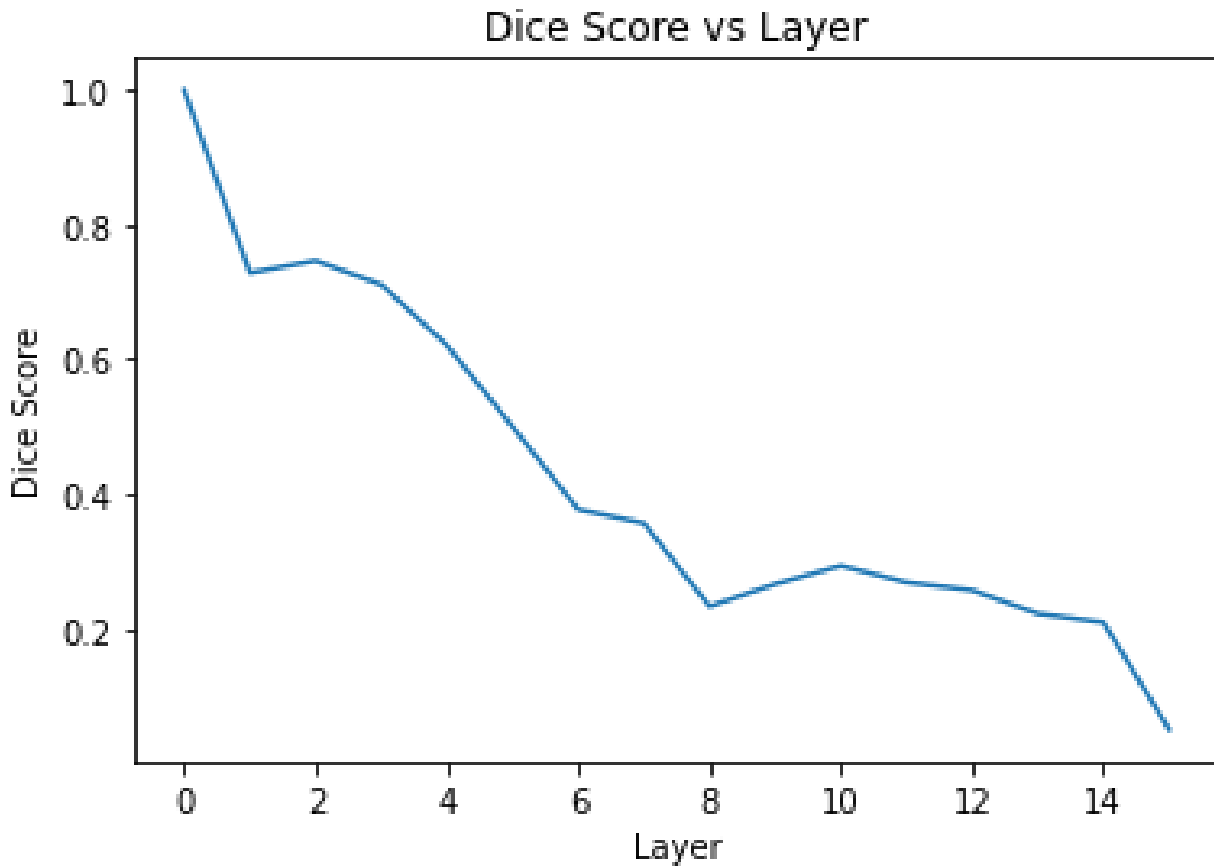


Figure 8: Dice score vs layer for area functional design

The functional seen in Equation 5 was incorporated into the design to penalize arc length. Another trial was conducted using the new design with both functionals and the test file. The results of this trial can be seen in Figure 9. The plot of dice scores can be seen in Figure 10. The average dice score was 0.505, an improvement of 0.077 compared to the previous design iteration. The arc length penalty improved the average dice score of the design and resulted in the later contours produced by the algorithm to be less complex, as desired. However, the contour produced by the algorithm is still quite far from the ground truth and the average dice score of 0.505 indicates that there is still significant room for improvement.

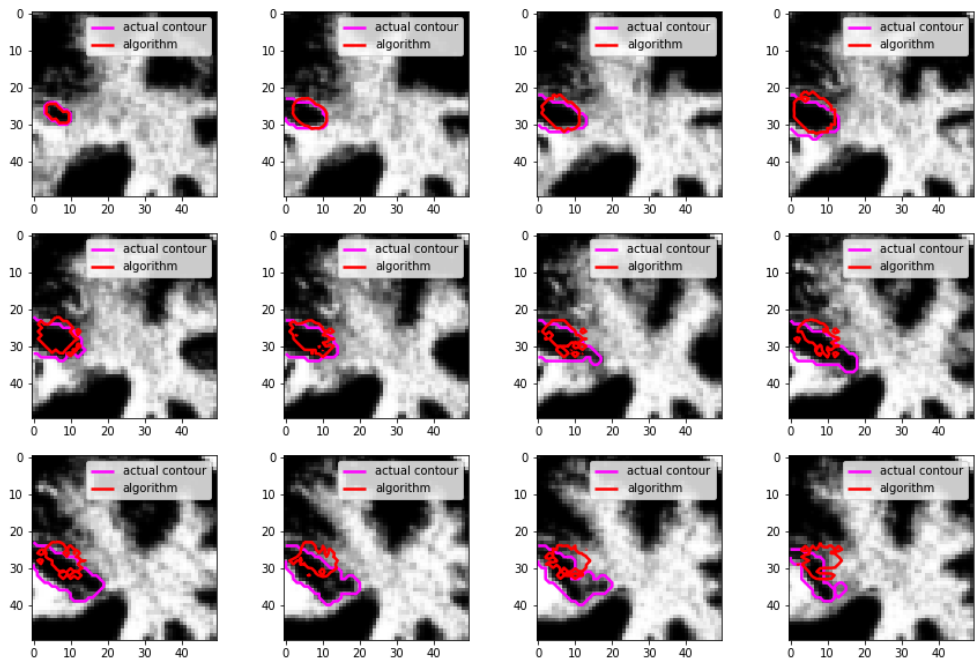


Figure 9: Algorithm output using area and arc length functionals

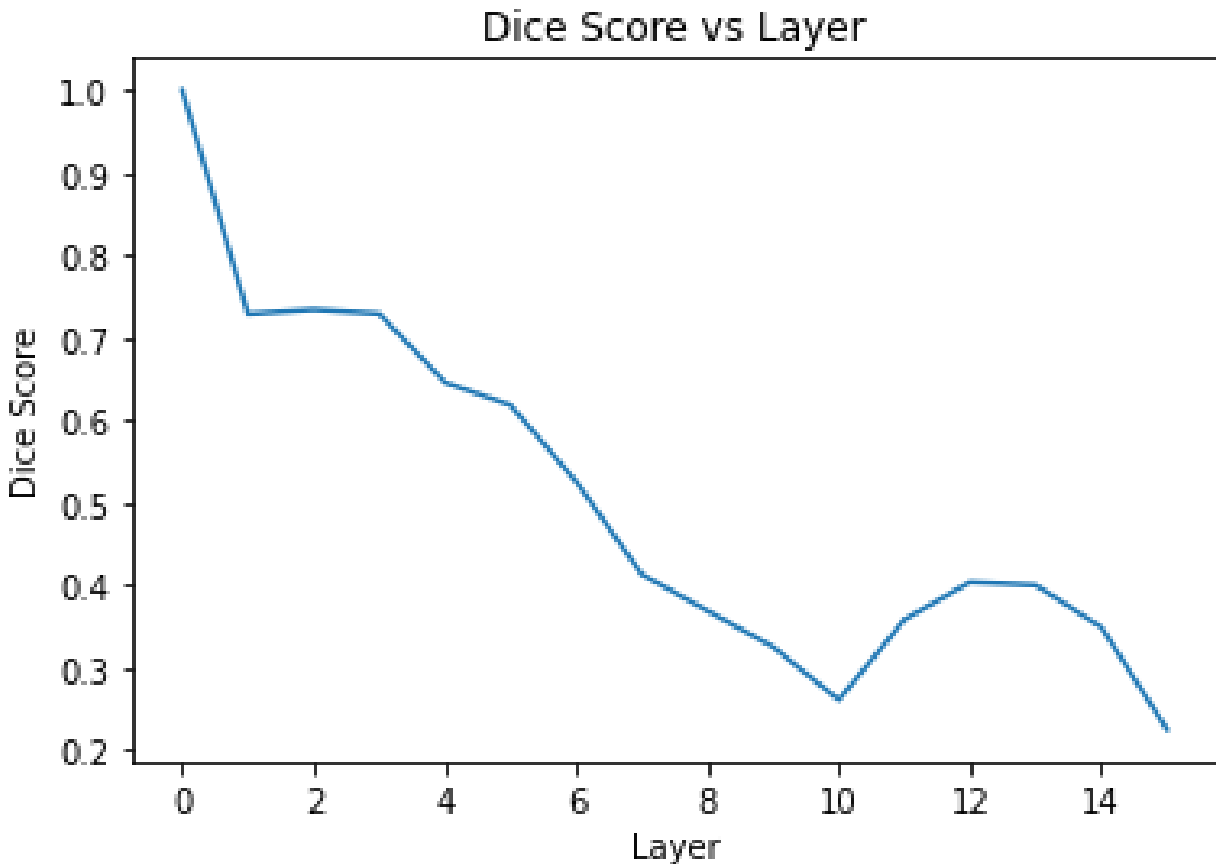


Figure 10: Dice score vs layer for area and arc length functionals design

The contours produced by the algorithm in these trials were close in size to the ground truth but were not entirely correct in shape and location. This indicates that area and arc length posses some information but not enough to fully track the region of interest.

4.5.2 Average Intensity Invariance based Design

From the data exploration conducted previously in the design process, it was determined that the average intensity within a lesion did not change significantly between layers. Area and arc length were insufficient as a basis for the algorithm used in the previous iteration of the design. Trials were conducted using the functional seen in Equation 11 to determine if the design could be improved with the use of a functional based on average intensity. The arc length functional was included in the design to prevent the algorithm generating excessively complex contours as in Figure 7.

A trial was conducted using this design and the test file to produce Figure 11. The plot of dice scores can be seen in Figure 12. The average dice score was 0.542, an improvement of 0.037 compared to the previous design iteration. The contours produced by the algorithm are in the correct location and are generally the correct shape. The main flaw with this design iteration is the contours produced by the algorithm generally being smaller than the ground truth.

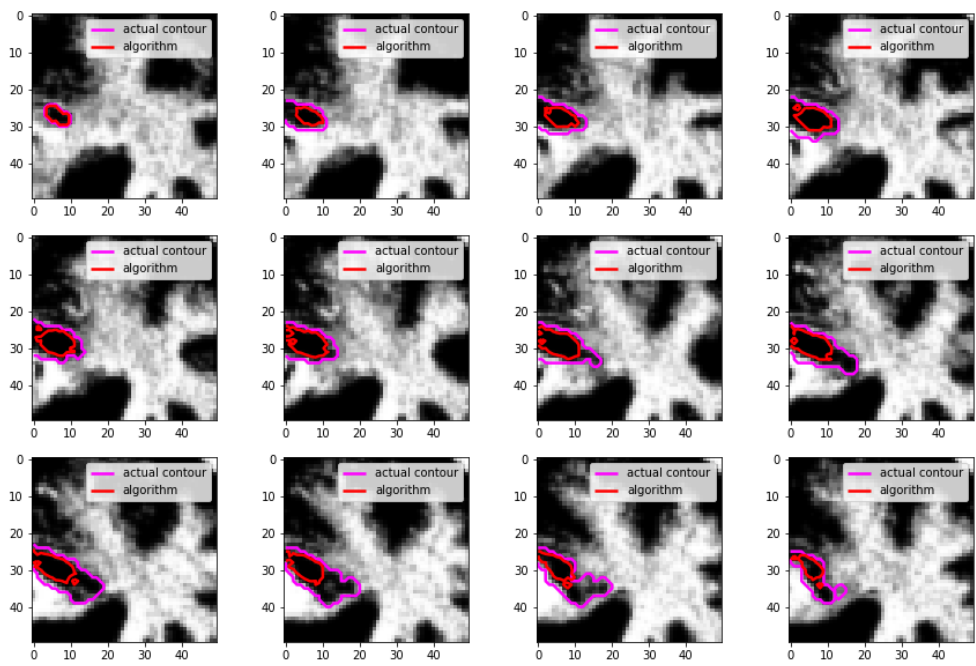


Figure 11: Algorithm output using intensity and arc length functionals

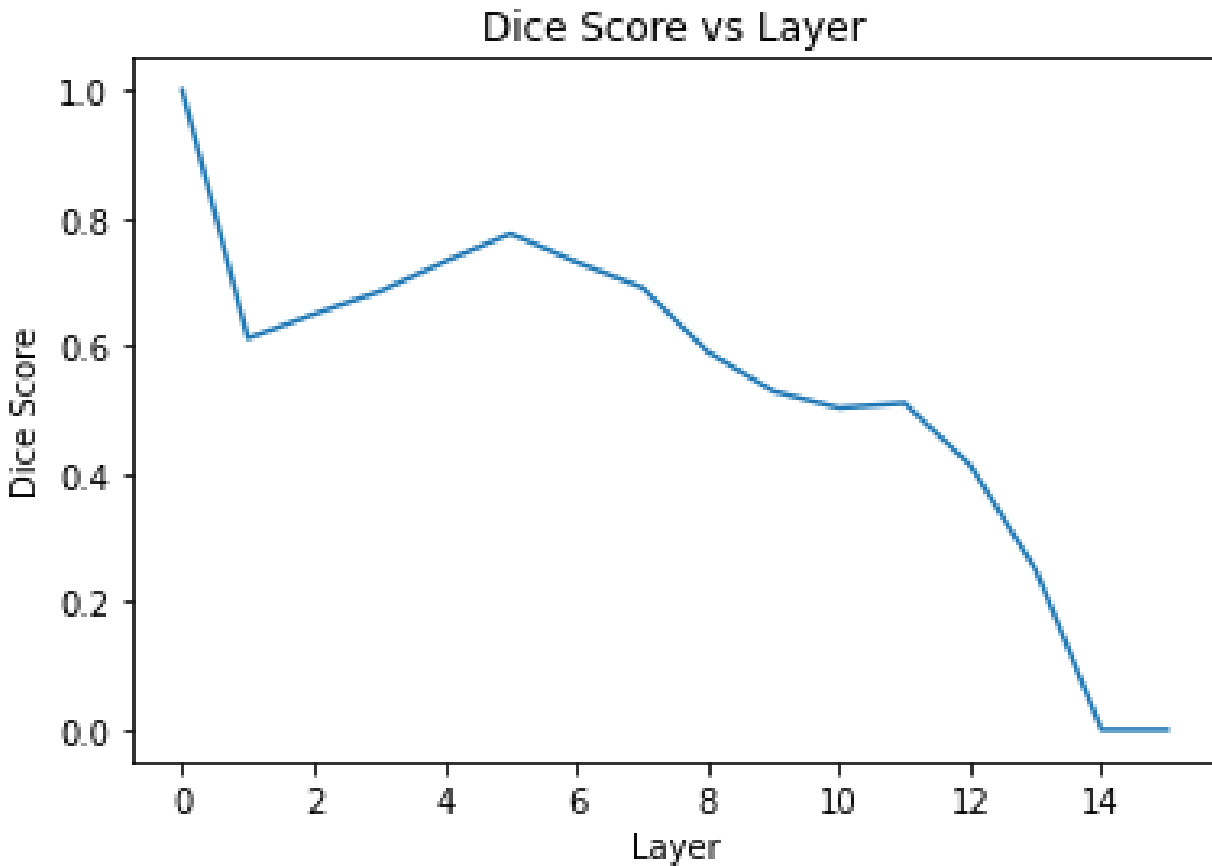


Figure 12: Dice score vs layer for intensity and arc length functionals design

Trials conducted with other files in the data set displayed a flaw with this design in which the algorithm struggled to produce accurate contours when there were large intensity changes between layers. Figures 13, 14, and 15 show a sequence of successive layers in a file with the algorithm generated contour and ground truth. Between layers, the lesion expanded but the intensity in the new region was lighter than in the original region. The algorithm was unable to account for this and expanded into the darker regions of the image, which correspond to the folds in the brain.

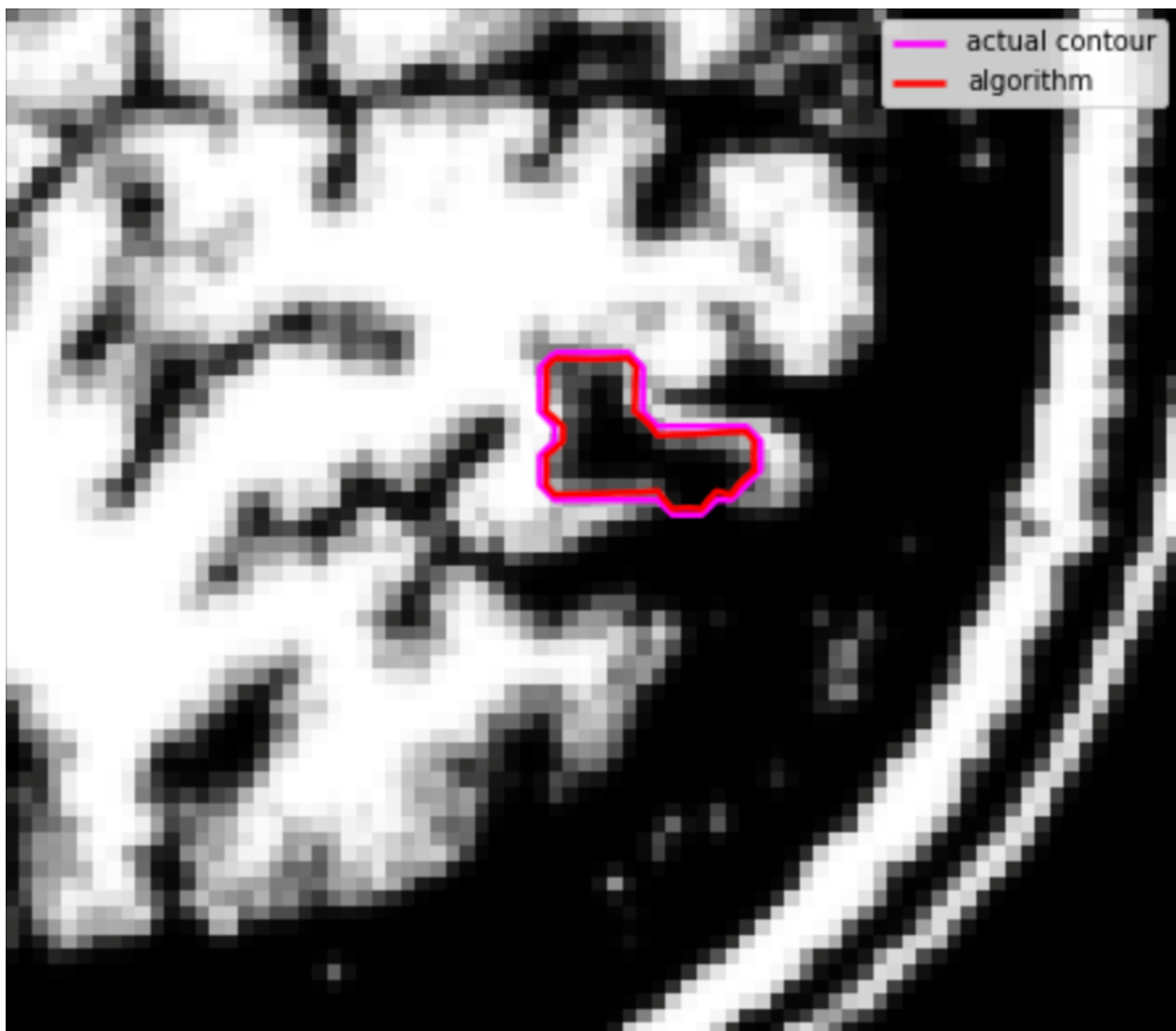


Figure 13: First image in a sequence using intensity functional

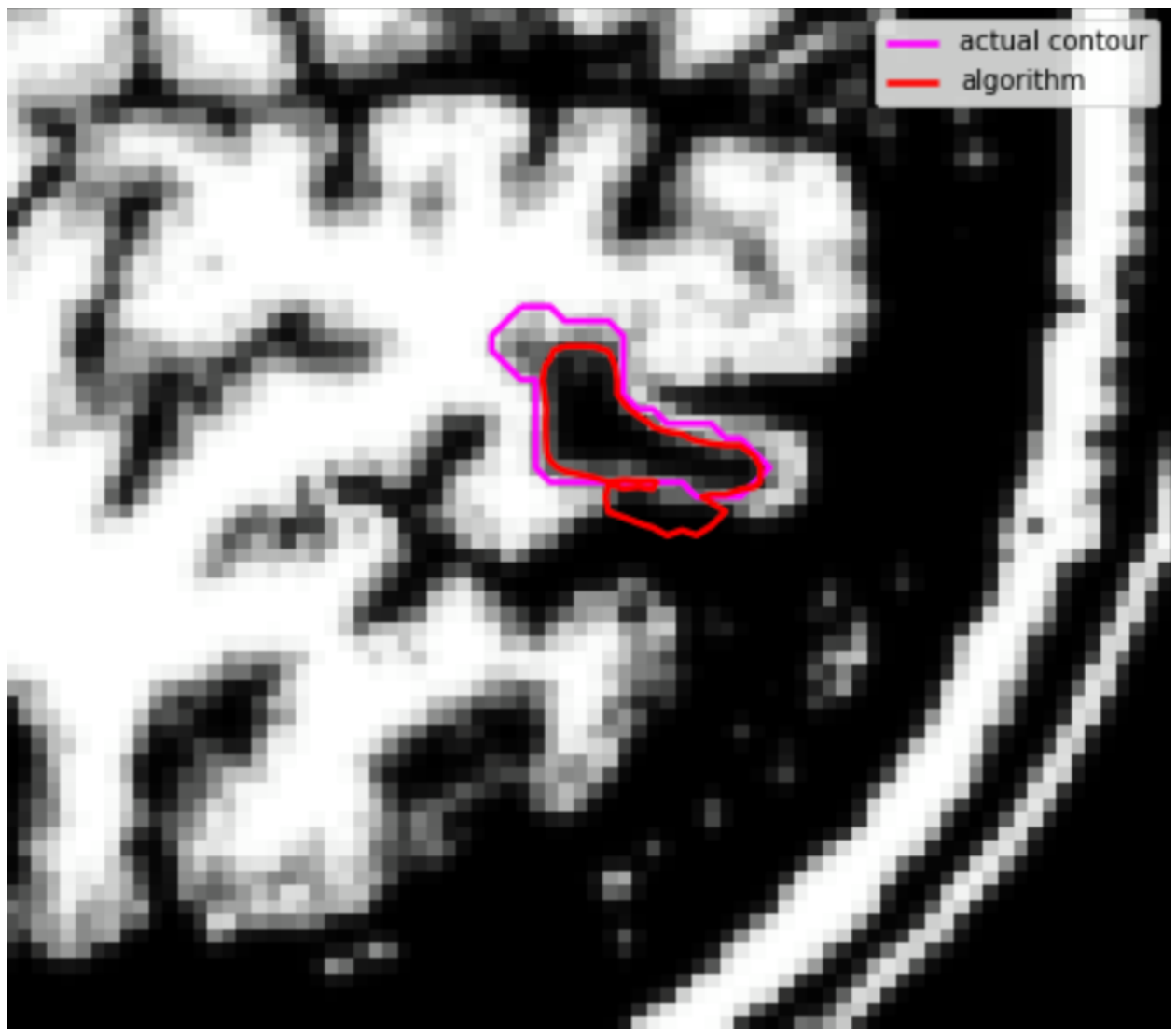


Figure 14: Second image in a sequence using intensity functional

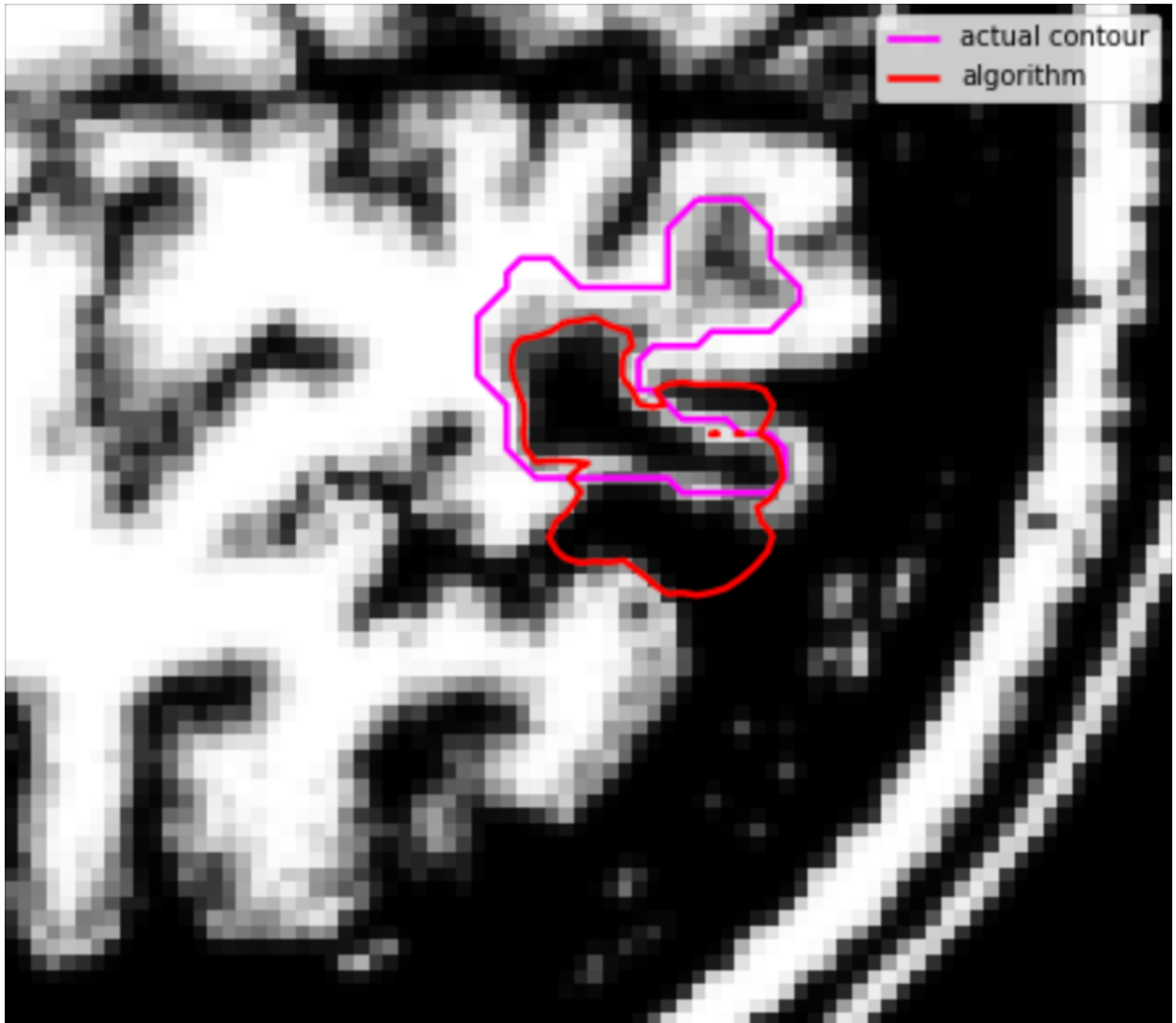


Figure 15: Third image in a sequence using intensity functional

These trials showed that the design based on intensity and arc length were somewhat successful. The contours produced by this iteration of the design tended to be the correct shape in the correct location but were generally not the right size. In contrast, the previous design based on area and arc length produced contours of the correct size, but incorrect shape and location. As such, the final design should incorporate intensity, area, and arc length to maximize the amount of information that can be used.

4.5.3 Image Pre-Processing

From the initial data exploration and experimentation, it was found that the boundary between lesion and other brain tissue was unclear. As well, there was noise present in the images that would cause problems for the algorithm. As such, the images needed to be processed to increase contrast and reduce noise. Histogram equalization was selected as a potential technique to increase the contrast of the images with the goal of making a sharper border between the lesions and the healthy tissue.

Histogram equalization is an image processing technique that transforms the intensity values for the pixels so that the empirical distribution function of the intensity values resembles the cumulative distribution function for a uniformly distributed random variable [16]. Shown below in Figure 16 is the histogram of intensity values for an MRI layer prior to histogram equalization. Figure 17 shows the histogram of intensity values for the image after histogram equalization was applied. An example of an image before and after histogram equalization can be seen Figure 18 with the former on the left and the latter on the right. Although histogram equalization did notably increase contrast in certain images, it was determined that this approach would not be suitable for the MRI images in this project. Figure 16 shows a clear skew towards intensities near zero in the image and as a result, histogram equalization was ineffective at flattening the histogram for the output image, as seen in Figure 17.

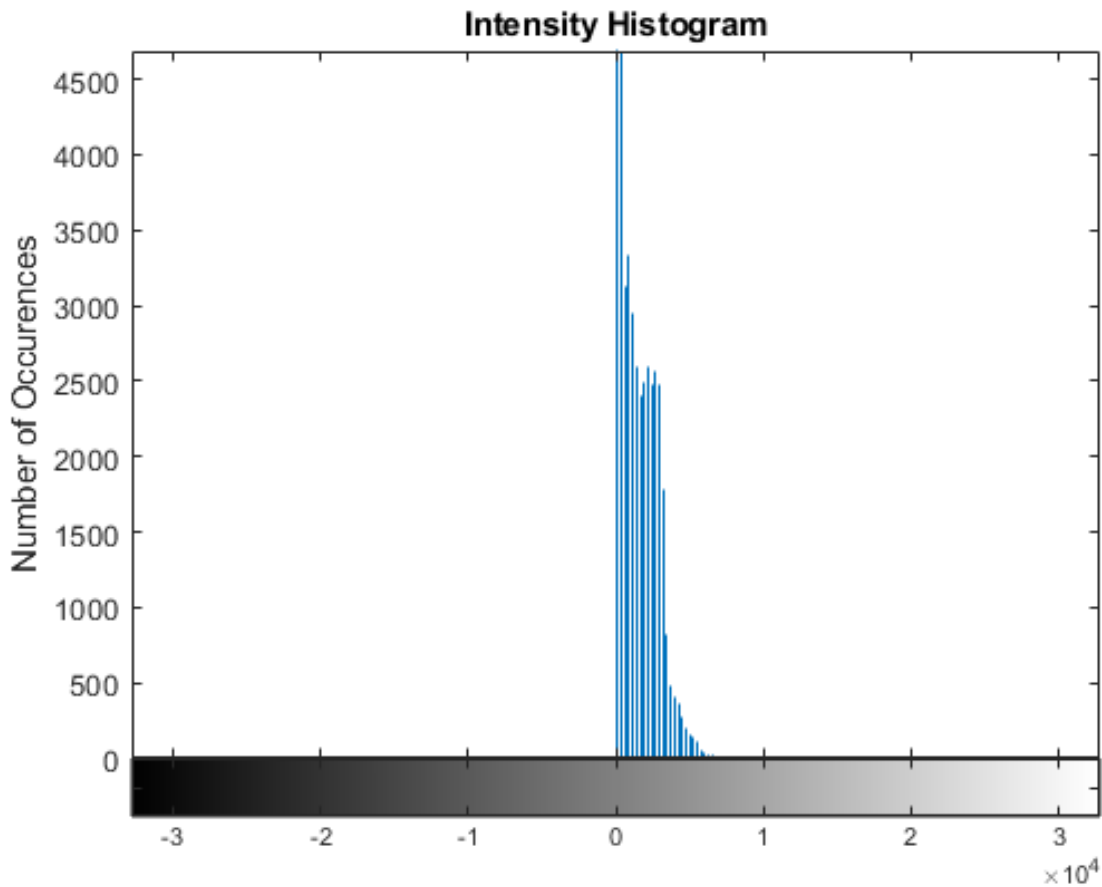


Figure 16: Intensity histogram of image prior to histogram equalization

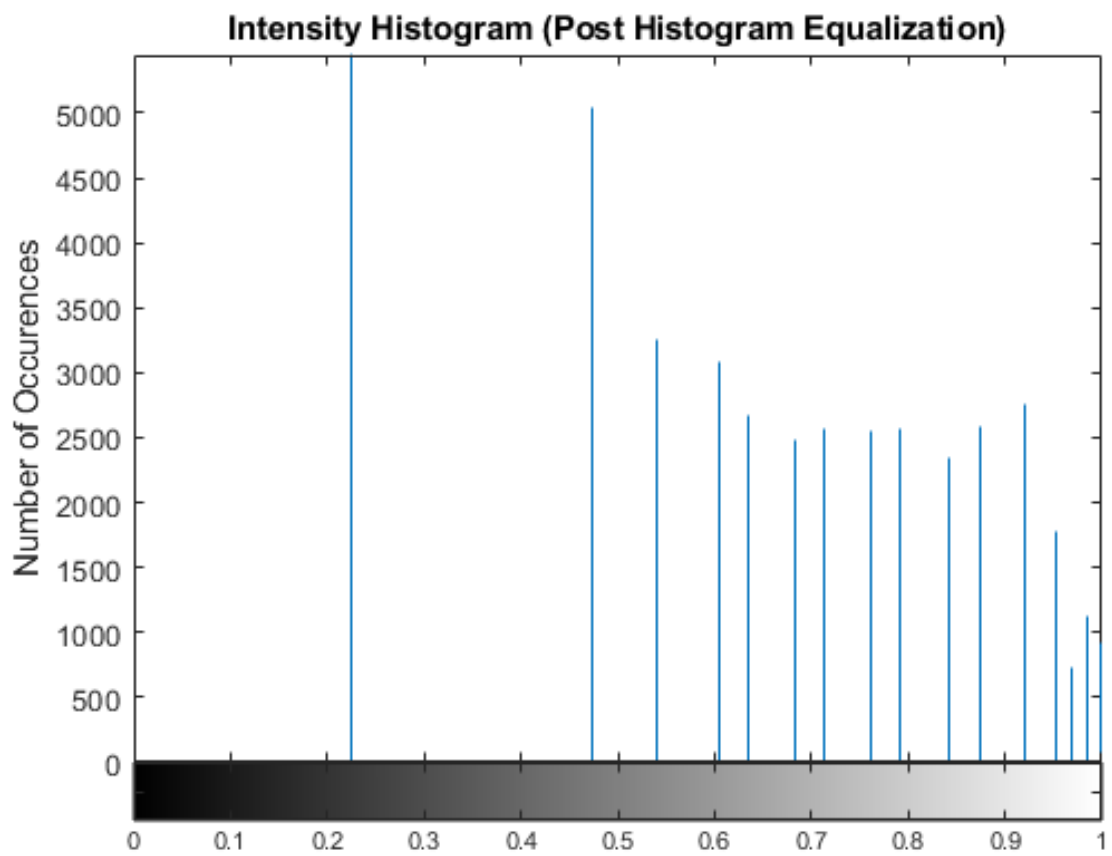


Figure 17: Intensity histogram of image after histogram equalization

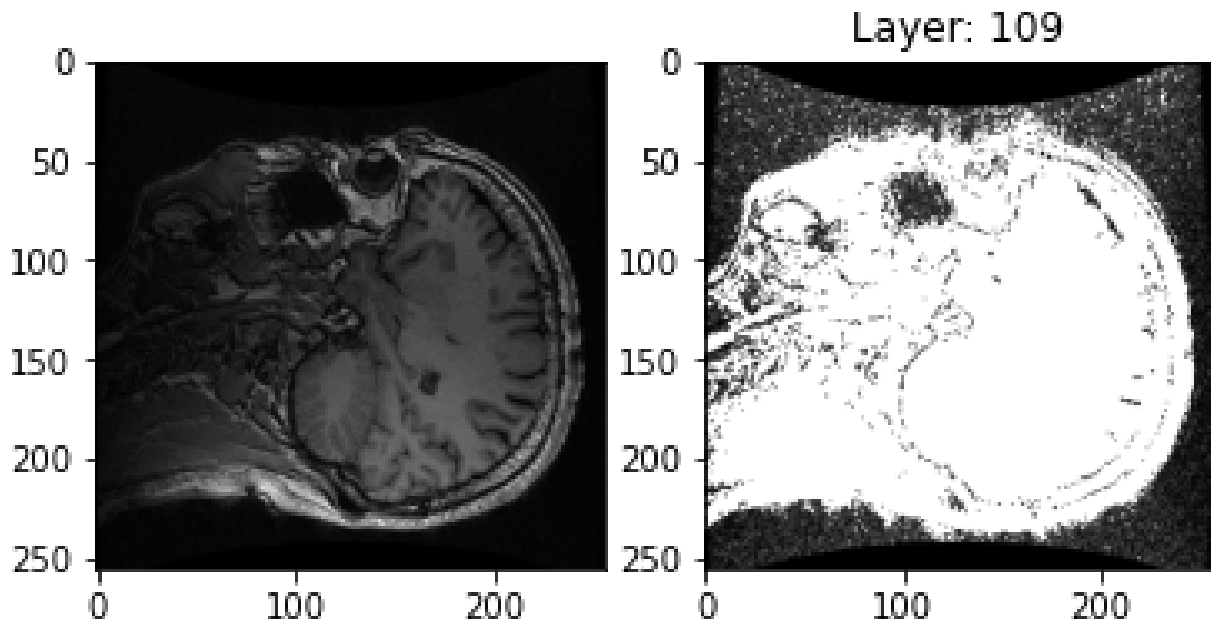


Figure 18: MRI image prior to histogram equalization (left) and post histogram equalization (right)

To increase contrast in the images, the Python library Pillow was used. After testing various values, the contrast factor was set to 12. To reduce noise, a Gaussian blur was applied with a radius of 0.6. When contrast was not increased and noise was not reduced, the design based on arc length and intensity used with the test file produced an average dice score of 0.114. When the image processing was applied, the average dice score was 0.542. This showed that if a functional based on intensity was to be used in the design, image pre-processing would be vital. As well, the scale of the improvement indicated that the choices of contrast factor and Gaussian blur radius were appropriate. Figure 19 shows a segment of one layer of the test file before the image processing was applied and Figure 20 shows the same segment after the image processing was applied. The lesion in the segment is traced in red.

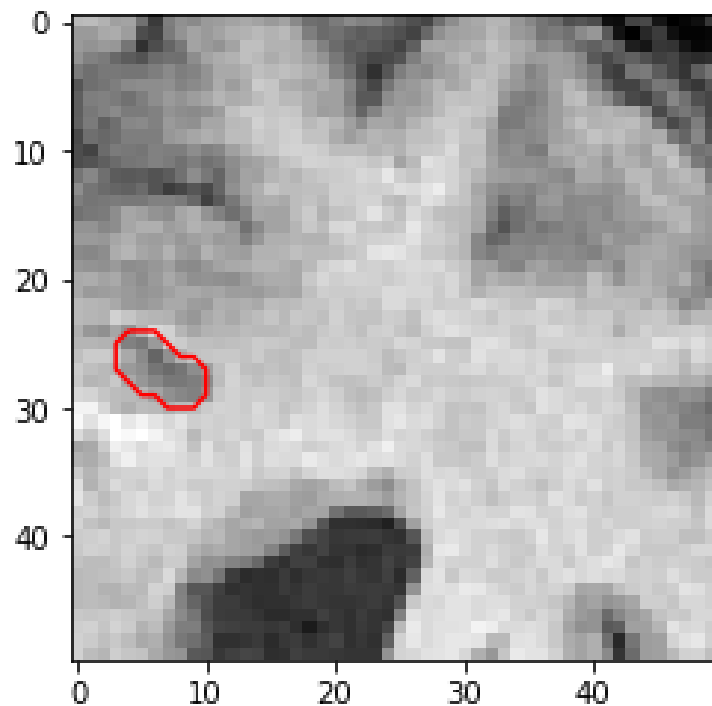


Figure 19: Image segment before pre-processing

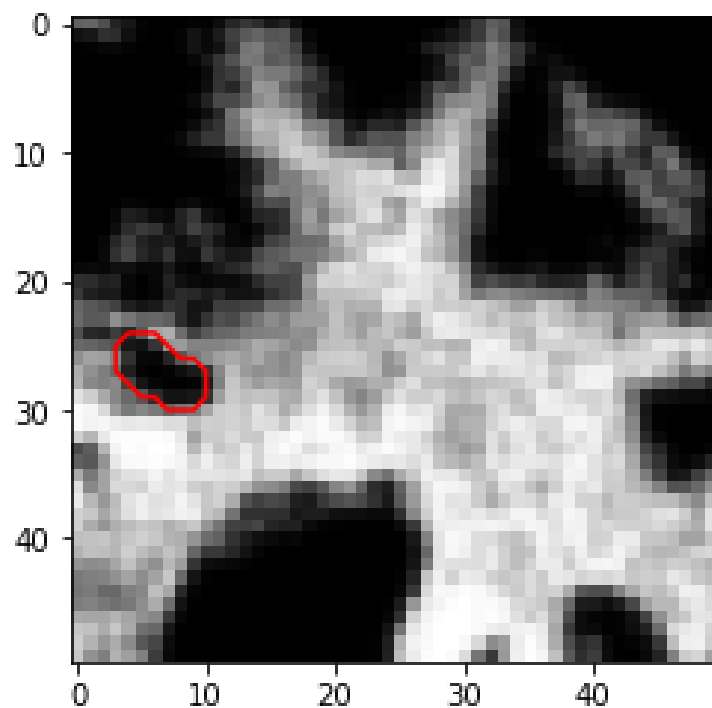


Figure 20: Image segment after pre-processing

5 Design Solution

5.1 General Solution Description

The final solution for the engineering challenge of brain lesion identification and tracking consisted of a code repository with a main script for executing the algorithm. Specific features of the repository include a "contour" class which facilitates the implementation of the Level-Set PDE, an image pre-processing pipeline that improves computation time and algorithm performance, a region tracking algorithm using history, and high-level utility math functions.

The operation of the lesion algorithm is procedural and can be understood through the following steps:

1. A medical professional outlines the brain lesion in the first image.
2. MRI scans and the identified reference lesion are provided to the algorithm at initialization.
3. Image pre-processing is implemented to reduce scan dimensionality and improves lesion visual distinctiveness.
4. An initial contour object, c_0 (a surface), is iterated until its zero level set matches the reference scan outline using a basic segmentation functional for the updates.
5. A new contour object is instantiated with a functional which is tuned using information from the previous image(s). This new surface, $c_k(t)$, $k \in [1, \text{length}(\text{scans})]$ is such that at $c_k(0) = \lim_{t \rightarrow \infty} c_{k-1}(t)$, i.e. the new surface at time zero matches what the previous surface converged to.
6. c_k is iterated until convergence.
7. Steps 5 and 6 are repeated until all scans have been analyzed
8. Images with the predicted lesion outlines superimposed over the original MRI scan are generated

The design solution also provides the option for supervision in the early stages. In this scenario, a medical profession observes the first few lesion identification processes and provides corrective feedback to the algorithm. This input results in more finely tuned parameters in the model and consequently the algorithm produces more accurate results. As low as three supervision stages have shown significant performance gains in the algorithm.

5.2 Assumptions and Approximations

It is assumed that the image will have grey scale and not colour values. If the input images had colour, the colour space would need to be reduced to black and white in the pre-processing stage. This would limit the amount of information our algorithm has access to, but in practice would offer significant time speed-ups since each image would only have one third the original data. Here it is assumed that the grey scale intensity alone is sufficient to describe the color properties of the lesion in a useful manner.

In concerns to lesion properties, it is assumed the average intensity inside and outside the lesion are invariant throughout the scans. Additionally it is assumed that lesion area in a specific layer can be faithfully estimated using a polynomial regression model fit with the area information from previous layers. In the early stages of the algorithm, polynomials of degree 0.5 have been

shown to model the area estimates accurately.

In the scope of this project it is assumed that the indices of the first and last images which contain the lesion are known. This assumption facilitates the testing and design processes, though is not required in practice.

5.3 Functional

The functional implemented to accomplish the task of lesion identification and tracking relies on three sub-functionals which accomplish arc-length minimization, image segmentation, and area prescription. It is the combination of these last two terms which perform the identification task, the first term being included to ensure solutions are smooth and also to help increment the level-set should the intensity and area terms have negligible effects over some transient period.

Explicitly, the functional takes the form

$$E[\vec{\gamma}] = a_1 E_1[\vec{\gamma}] + a_2 E_2[\vec{\gamma}] + a_3 E_3[\vec{\gamma}] \quad (17)$$

where

$$E_1[\vec{\gamma}] := \oint_{\vec{\gamma}} ds \quad (18)$$

$$E_2[\vec{\gamma}] := \int_{R_{\vec{\gamma}}} (I(x, y) - \mu_i)^2 - \int_{R_{\vec{\gamma}}} (I(x, y) - \mu_o)^2 \quad (19)$$

$$E_3[\vec{\gamma}] := \left(\int_{R_{\vec{\gamma}}} dA - A^* \right)^2. \quad (20)$$

Here, μ denotes intensity with the subscript referring to either inside or outside the region enclosed by the contour, I is the image, and A^* is the magnitude of the area we wish our contour to converge to. Additionally, coefficients c_i denote the proportions in which we combine the three functionals.

The effect of E_2 is that our surface will evolve in a way which seeks to maximize the number of pixels with intensity μ_i enclosed within the contour region which means the surface can become quite irregular. The arc-length minimizing term helps mitigate some of these side effects, while the functional E_3 ensures the region enclosed by the zero level set will not become too large. Since the area functional relies on the term A^* which is a regression estimate, we take the coefficient a_3 to be smaller than a_2 to account for the inherent uncertainty.

Testing the functional on MRI images revealed an optimal ratio of coefficients to be $a_1 = 0.005a_2$ and $a_3 = 0.3a_2$. Here it can be seen that the image segmentation functional plays the largest role overall. Specific values for these coefficients used in the execution of the code were $a_1 = 0.0003$, $a_2 = 0.06$, and $a_3 = 0.02$. This setup also corresponds to the case where the time step was taken to be $dt = 0.001$. The size of these coefficients is entirely dependent on the choice of time step and the convention by which surfaces are defined as the term $\|\nabla u\|$ appears directly in the level set PDE.

5.4 Results

The current algorithm has shown a promising capacity for the identification and tracking of brain lesions in MRI scans under mild constraints using a fairly simple functional.

After testing the algorithm against the previously discussed dataset, it was found that T1 weighted MRI's were best suited for the application purposes. This is due to the fact that lesions were more visually apparent in this MRI convention meaning segmentation was facilitated at the outset. Image processing further stressed key features such as lesion borders and image intensities thus adding to this.

Returning to the discussion in Section 4 where the effects of different functional terms were discussed, it can now be seen how the final functional performs on the same set of MRI scans.

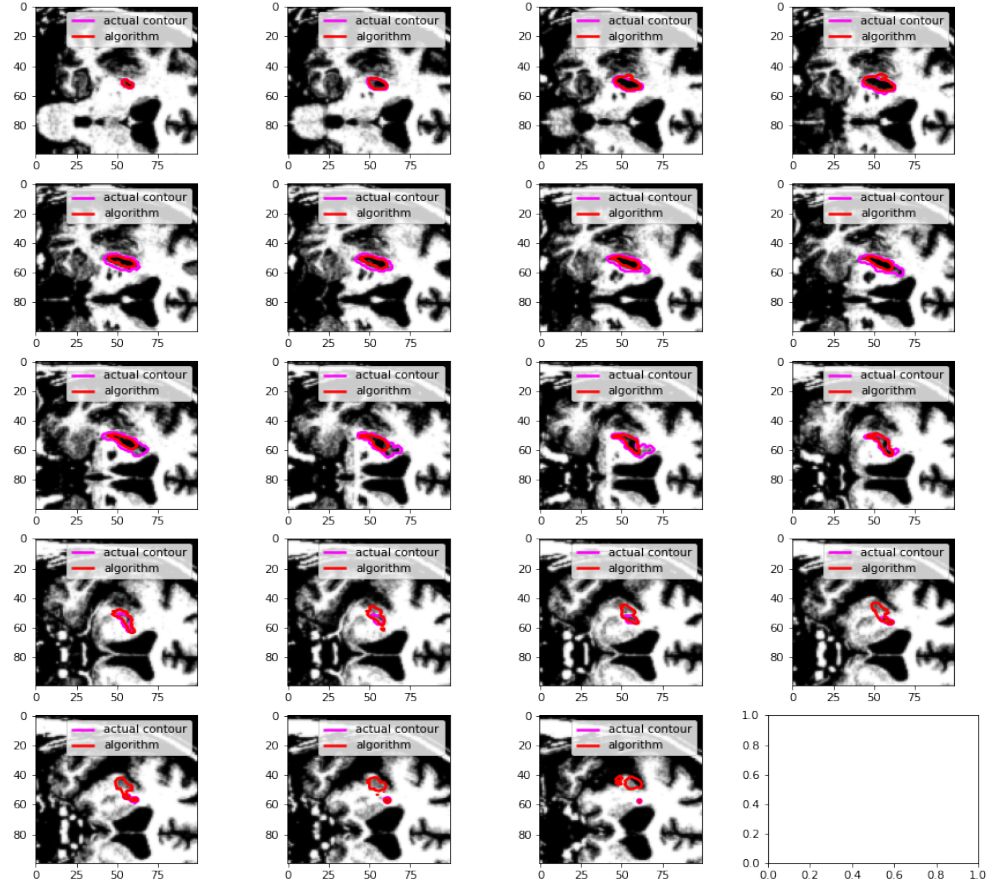


Figure 21: Finalized algorithm performance on benchmark scans

The above represents a much more faithful identification of lesions in the data set than earlier unrefined attempts, and serves as a testament to the merit of this approach for the automation of lesion labelling. Additionally, our ability to generate such a collection of images in a time-efficient

manner meets of the main goals of the project outlined in the Problem Description. More detailed assessments of the algorithm's performance will be discussed in upcoming sections.

The effect of image processing on the performance of the algorithm is directly seen when comparing the results of the previous figure to the output generated in the case where no image processing is performed.

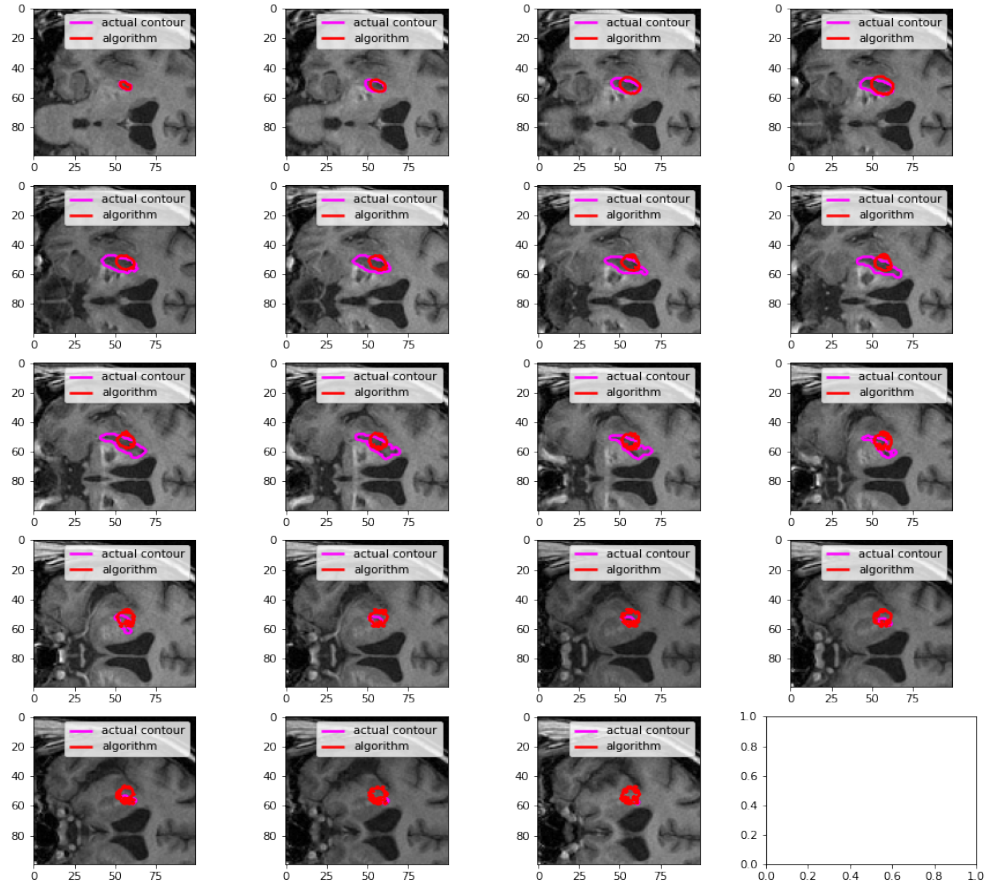


Figure 22: Finalized algorithm performance on benchmark scans, no image processing

Here, the algorithmic contours do not capture many significant lesion properties and simply exist within a close region to the actual target. This illustrates that in order to use the relatively naive functional here presented, image processing is essential.

Another important factor to discuss is the effect of supervision in the operation of the algorithm. Here, supervision refers to the corrections made to the area regressor estimates for functional

E_3 which are obtained in practice from a supervising medical professional. In order to adequately fit the polynomial regression model, assume supervision for the first 4 scans. After this the code is entirely self run. Consider now the algorithm run using supervision for only 2 runs on pre-processed images.

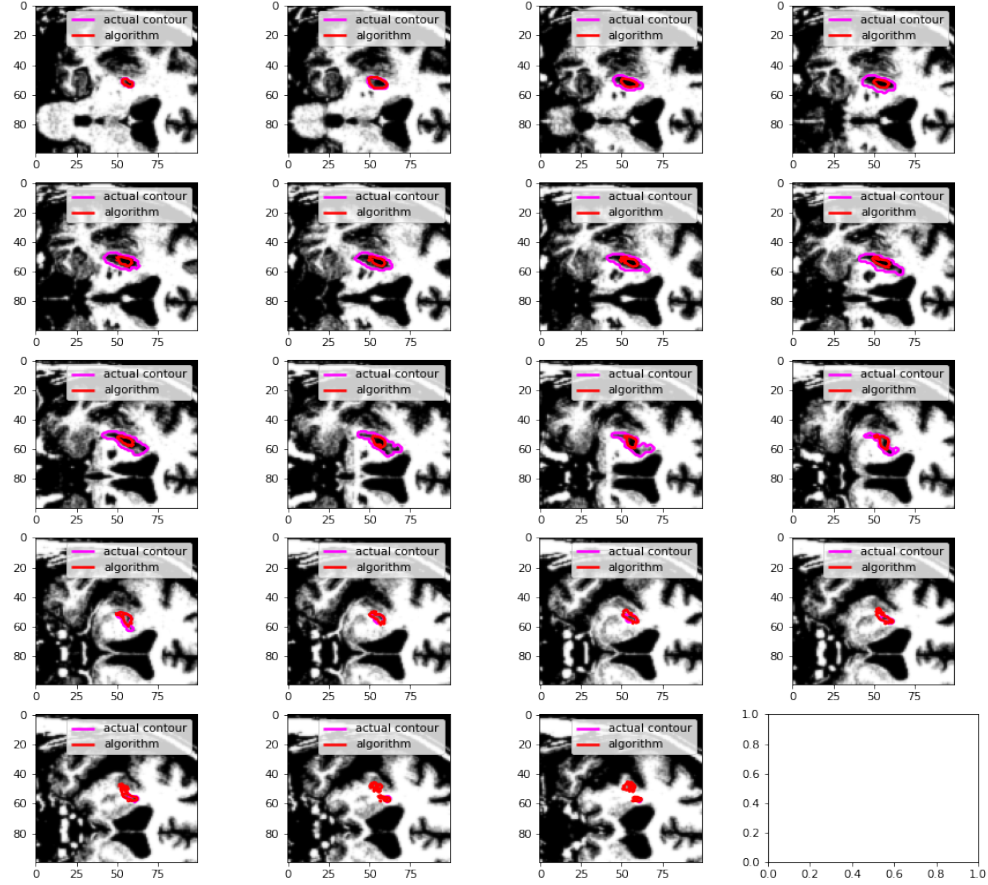


Figure 23: Finalized algorithm performance on benchmark scans, supervision for 2 stages

Although the differences between this series of scans and the ones previously presented are subtle, one can clearly see how the algorithmic contours do not capture the lesion borders in many of the intermediary slices. In the aggregate, this lack of supervision results in a series of outlines which are not as accurate as the ones obtained using greater supervision.

5.5 Solution Limitations

Throughout testing, it was found that the algorithm only produced viable results for certain MRI data sets. Necessary conditions for these sets were high contrast between the lesion and the

surrounding matter, no holes in the lesion, and small variance in intensity, shape, and position from slice to slice. The algorithm is also only tuned to lesions caused by strokes, otherwise known as vascular lesions. Other types of lesions have specific shapes and intensities associated with them, so there is no guarantee that the algorithm created will work for any other type of lesion. Finally, the process is not fully automatic since it requires a specialist to segment the first lesion slice. This results in the algorithm not being as efficient or convenient as originally planned.

6 Implementation Evaluation

6.1 Solution Evaluation

6.1.1 Total Average Runtime

The time it took for the algorithm to complete a single segmentation ranged from 6 to 8 s depending on the size and complexity of the MRI lesion slice. It is important to note that this range will change depending on the processing power and RAM of the computer the algorithm is run on. The lesions tested for the purposes of runtime varied in number of slices, ranging from 9 to 44. This would result in computation times between 36 s and 352 s depending on the lesion's size per slice and the depth of the lesion. It was found that the average runtime for just the algorithm was approximately 140.7 s. After adding 120 s for the initial manual segmentation to this time, the total average runtime was computed to be 260.7 s.

6.1.2 Average Dice Similarity Coefficient

The average DSC was computed for six different lesions. Table 7 and Table 8 represent the DSCs per slice in a given image set and the average DSCs for each image set, respectively.

Table 6: File legend for Table 7

File Name	Corresponding Letter
c0001s0012t01	A
c0002s0004t01	B
c0002s0014t01	C
c0002s0016t01	D
c0002s0027t01	E
c0001s0006t01	F

Table 7: DSC values per slice

Slice Depth	A	B	C	D	E	F
1	1.0	1.0	1.0	1.0	1.0	1.0
2	0.78947	0.92307	0.73333	0.62857	0.6875	0.79310
3	0.55760	0.87	0.58333	0.63043	0.46666	0.65625
4	0.49523	0.84848		0.80952	0.16666	0.47916
5	0.53809	0.84848		0.46153	0.13333	0.38261
6	0.55327	0.69642			0.52173	0.10053
7	0.53526	0.69026			0.69230	0.08071
8	0.47204	0.66666			0.47619	0.07926
9	0.32109	0.62650			0	0.08185
10	0.29226	0.65822			0.14285	0.09090
11	0.23993	0.67942			0.38888	0.08264
12	0.21779	0.8			0.48648	
13	0.20172	0.61788			0.64516	
14	0.19204	0.42307			0.38709	
15	0.18401	0.38383			0.32558	
16	0.18424	0.31914			0.22727	

Table 8: Average DSCs

	A	B	C	D	E	F
Average DSC	0.42338	0.68278	0.77222	0.70601	0.42173	0.34791

As seen in Table 8, the average DSC for a lesion can range from about 0.34 to 0.77 and averages around 0.55. Looking at Table 7, the DSC generally decreases the further the lesion slice is from the professional’s segmentation. This leads to lesions that were smaller in depth to have larger DSCs. The decrease in DSC could be due to compounding errors from previous iterates since the algorithm designed bases its current segmentation on the one previous. Another factor could also be the varying sizes and complexities from slice to slice. It was found that the more a lesion varied in area, arc length, and intensity from slice to slice, the larger the decrease in DSC.

6.2 Compared to Existing Solutions

6.2.1 Manual Segmentation

Assuming that the average amount of time it takes for a specialist to segment one lesion slice is two hours and given the algorithm’s average runtime, 115.5 minutes would be saved. The algorithm performs about 27.6 times faster than a specialist. The average DSC being 0.55 means that about half of the algorithm’s segmentation contains pixels corresponding to a lesion and the other half contains pixels that are not associated with the lesion. Visually, it was found that the algorithm’s segmentation surrounded the lesion in question as well as portions of the scan around the lesion. This means that, while the algorithm’s segmentation may estimate that the lesion is larger than it actually is, it crucially does not generally cut out parts of the lesion from its segmentation.

6.2.2 Existing Auto-Segmentation Algorithms

Three existing auto-segmentation algorithms were chosen to evaluate the team’s algorithm’s performance. They were ALI, lesion_gnb, and LINDA. The values for average runtime and average

DSC were taken from a study evaluating these algorithms using lesions from strokes [12]. The data collected is summarized in Table 9 below.

Table 9: Comparison of region tracking algorithm to existing software

	ALI	lesion_gnb	LINDA	Region Tracking
Average Runtime (s)	396.99	246.12	3843.66	270.6
Average DSC	0.40	0.42	0.50	0.55

From the data, the algorithm created by the group produces results comparable to existing auto-segmentation algorithms. However, it is important to note that the data set used to evaluate ALI, lesion_gnb, and LINDA was different and larger than the one used to evaluate the group's algorithm. It is also important to mention that the data sets chosen for testing in this project were subject to specific criteria, such as no holes and no large variances in shape or intensity. This is probably the reasoning behind the team's algorithm appearing to have the highest DSC out of all of them. Therefore, the results shown in Table 9 may not be an accurate representation of how well the team's algorithm performs against existing competition.

7 Triple Bottom Line Impacts, Ethics, and Economic Analysis

7.1 Social Impacts and Considerations

MRI machines are the second most common type of medical imaging technology in Canada, having 366 machines as of 2017 [17]. They are also the most heavily used, running 78.7 hours per week in 2017. Given that an MRI test can take between 15 and 90 minutes to complete, there is an average of 11.24 MRI scans per day [18]. Although an experienced radiologist or other specialist may not need to segment every MRI image set to make initial diagnoses, segmentation is often required to give the medical professionals quantitative information for the area in question [19]. Since the average time it takes to manually segment an MRI image set is two hours, medical professionals would approximately have 22.5 hours-worth of images to segment per day [20]. In comparison, the auto-segmentation algorithm created only takes an average of 270.6 s to fully segment an MRI brain lesion. Although not all MRI scans performed in a day are going to involve brain lesions, radiologists and specialists can still save around 115.5 minutes for each MRI image set with a brain lesion. The increase in time-efficiency allows these specialists to spend more time performing diagnostics and caring for their patients. This will lead to smaller diagnostic wait-times, increased patient satisfaction, higher patient discharge rates, and increased control over influxes in high-priority patients.

Researchers will also be able to benefit from the increase in time-efficiency. The ability to segment more MRI datasets within a given timeframe allows researchers to use larger sample sizes in their studies. This is important for increasing reproducibility, which can help create standards for diagnostics and treatment. In the biological field, this is extremely important since the human body can vary drastically from person to person.

Governments and health organizations may also be affected by this technology. Auto-segmentation software falls under the International Medical Device Regulators Forum's (IMDRF) definition of software as a medical device [21]. The IMDRF has also published a general guideline outlining how software as a medical device should be regulated. However, there are currently no international quantitative regulations since the range of software is diverse and each will need different metrics

of evaluation to guarantee safety. Concerning Canada specifically, software as a medical device is regulated under the Food and Drugs Act [22]. This document regulates medical devices based on a risk versus scope analysis, but again does not have any quantitative measures. As medical software becomes more prevalent and accurate, governments and health organizations will have to adapt accordingly to ensure the safety of patients.

7.2 Standards, Codes, and Ethical Considerations

When designing and implementing the solution a number of ethical considerations were made and a variety of applicable standards and codes were followed. Additionally, relevant codes and standards must be followed by individuals once the software is implemented. When the initial problem scope was decided, the solution was determined to be an assistive tool for radiologist to use, instead of replacing radiologists and being the only thing tracing the lesions. The solution also requires the radiologist to trace the initial lesion, it can increase the accuracy, and force the radiologist to still analyze the scans. Additionally, all radiologists that utilize this software must undergo the associated training on how to properly use the technology to ensure that the software properly traces the lesions. All three of these ensure patient-centered care, which is a part of the CAMRT Member Code of Ethics and Professional Conduct [23]. When installing, calibrating and maintaining the software, and any required hardware, a field engineer must do so by abiding by their engineering code of ethics. This includes "[holding] the safety, health, and welfare of the public, [performing] services only in areas of their competence, [issuing] public statements only in an objective and truthful manner, [acting] for each employer or client as faithful agents or trustees, [avoiding] deceptive acts and [conducting] themselves honorably, responsibly, ethically, and lawfully so as to enhance the honor, reputation, and usefulness of the profession" [24]. In addition, the software must also ensure patient data is not leaked nor compromised, to abide by patient confidentiality. Overall, the solution reduces "harm from potential pitfalls and inherent biases", promotes well-being, distributes the benefits and harms among stakeholders in a way that respects human rights and freedoms, which includes privacy and dignity, and ultimately leaves the radiologist responsible for patient care, which abides the Ethics of Artificial Intelligence in Radiology [25].

7.3 Environmental Impacts and Considerations

If auto-segmentation was a limiting factor for the rate at which MRI scans are performed, then it would have a minor negative effect on the natural environment [26]. However, the current limiting factor for MRI scan rate is the availability of the MRI machines. Therefore, auto-segmentation is not correlated to the negative impact MRI machines can have on the environment at this time. Auto-segmentation does have a potentially positive impact on the natural environment by reducing the amount of time spent working on computers in hospitals. Depending on the type, a desktop computer can consume an average of 60 to 250 W when active [27]. When the desktop is on sleep or standby mode, the power consumption is decreased to about 1 to 6 W. If a specialist were to spend two hours manually segmenting an MRI image set, the energy consumption would be between 0.12 kWh and 0.5 kWh. If the auto-segmentation algorithm was used, the energy consumption would be between 0.0064 kWh and 0.030 kWh. This is an average savings of 0.29 kWh per MRI image set. The reduction in power consumption will help reduce the carbon footprint of hospitals, therefore positively affecting the natural environment.

With regard to a hospital environment, having a supportive environment was identified to be a key factor in making a hospital's environment patient-friendly [28]. The use of auto-segmentation algorithms will help build this supportive environment by giving medical professionals more time to

spend with their patients. The reduced diagnostic wait-times and higher discharge rates will also increase patient satisfaction and allow new patients to receive the treatment they need sooner. All of the mentioned factors will positively affect a hospital's environment.

7.4 Economic Impacts and Considerations

The algorithm could save approximately \$393.23 per MRI image set based on its average runtime and the average hourly wage for a radiologist in Canada [29]. These savings would be applicable to both hospital administration and researchers hiring specialists for the purposes of segmentation. Based on the calculations done in the previous section for power consumption and taking the average Canadian electricity pricing to be 0.112 CAD per kWh, the amount of money saved per scan is \$0.03 [30]. It was decided that the algorithm is going to be free to use in general. With that being said, there will be a training program offered for a flat fee of \$1000 per person with discounts offered for students and researchers. This design and pricing was based off of a training course for FreeSurfer, which is another free auto-segmentation software [31]. This fee will be mandatory if the algorithm is to be used for clinical diagnoses in an effort to limit liability.

7.5 Economic Analysis

The global medical imaging analysis software market size was estimated to be about 2.4 billion USD in 2019 [32]. This is expected to grow by another 8.15% from 2020 to 2027. This shows the high demand for new medical imaging analysis software like the algorithm created. It also shows that the algorithm would most likely still be profitable in the years to come, which is important since it will take more time to fully develop the algorithm. The economic timeline for this algorithm can be broken into two stages. They are the initial developmental stage and the marketing and sale stage. In the developmental stage, there are two main economic considerations. The first is the cost of development. The average software developer in Canada has an hourly wage of \$25.24 [33]. Assuming that the developmental stage takes a year and the developers are going to be working eight hour days five days a week, the annual cost for one developer will be \$52,499.20. Since the algorithm is not computationally demanding enough to cost non-negligible amounts to run and does not require the purchase of new hardware or software, the costs associated with running the algorithm are considered negligible. The majority of MRI image sets found online have similar costing to the one that was used in this report. They are free to access after an application to use them has been approved. Since the algorithm can be worked on from home, there will also be no need to lease an office. There will, however, be costs associated with hiring a radiologist or specialist to segment the data sets since most of them do not come with the scans already segmented. The average hourly wage for a radiologist in Canada is \$204 [29]. The cost of paying for the software developers and specialists will be covered by the Scientific Research and Experimental Development (SRED) program [34]. This is a Canadian tax credit program which cover the salaries or wages of employees involved in the project. After the initial development stage, the team will apply for an Idea for Innovation grant from the Canadian government [35]. This will help the team conduct market research, enhance the technology, and will pair the team with a Canadian company to help with further development, marketing, and sales. Once this is complete, the team will move to patent the algorithm while beginning its early stage of sales. The patenting process in Canada requires an initial application fee, a maintenance fee, and a final fee [36]. If the development timeline of one year is followed, it can be assumed that the application for the patent will occur in 2022. The application fee will be \$407.18. Assuming that it will take at most four years to process the patent, the maintenance fees will cost \$150.00. The final fee will cost \$305.39. Therefore, the total cost

for patenting will be \$862.57. While this is occurring, the algorithm will begin to be introduced into the market. Since it is free to use, profit will be generated by the training course. Since we made the training course mandatory if the algorithm was going to be used for clinical diagnosis, the target market for sales would be medical professionals. There are around 2,100 radiologists in Canada and about 90 radiology residents graduating each year. The profit generated by training the current radiologists would be \$2.1 million. By training the subsequent radiology graduates, this will generate another \$90,000 each year.

8 Next Steps

One of the main limitations to the accuracy of the algorithm is that it is meant to work for any lesion in general. Improvements to the accuracy of this project can be made by specifying towards one type of lesion. This is because lesions of a specific type will share certain properties with one another which would allow stronger assumptions to be made, and better functionals to be developed. Metastases, for instance, have very distinct borders and very constant image intensity within the interior of the lesion. With this in mind, the first taken towards improving the project would be to begin studying the different types of lesion individually, and developing unique functionals for each type of lesion.

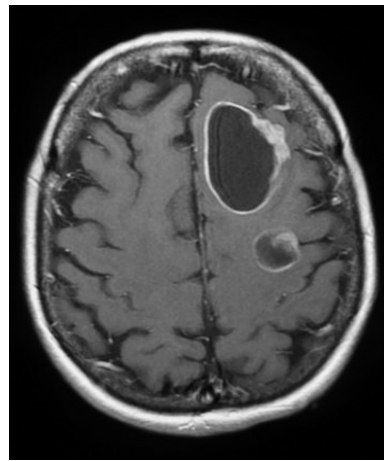


Figure 24: Metastasis with clear border and regular image intensity

Another step to making this project more generally useful is to continue to add functionality beyond lesion segmentation. Interviewing a radiologist also revealed some metrics that would be useful to have for developing radiotherapy treatment. For example, the total volume of the lesion or the smallest/largest distance between the lesion and the skull can drastically change which type of radiotherapy is administered.

At the beginning of this project the decision to work in Python was made due to the availability of useful math libraries and MRI processing libraries. The downside of using Python is that it has runtime issues. Given more time, resolving this issue would involve transcribing code into a language closer to the machine-level, like C++.

Finally, the most important step to making this project usable by professionals would be to develop a user interface. The GUI would make use of the additional research into individual types of lesions by allowing the user to select which type of lesion the program will be operating on. In addition, it

would be able to display the previously mentioned metrics (the volume of the lesion and its distance from the skull).

The addition of these features would result in a robust application usable by medical professionals.

9 Conclusion

The final design was based on functionals encoded with information about the expected area and average intensity of the lesion. As well, a functional was included to penalize arc length and reduce the complexity of the contours produced. From the experimentation and design process, it was found that the designs based only on area and arc length produced contours of the correct size and with smooth boundary, but were often in the incorrect location and the incorrect shape. As well, it was found that designs based only on average intensity and arc length produced contours that were in the correct location and were the correct shape, but were not the correct size. When all three properties were included in the design, their strengths were complimentary and the produced contours were quantitatively superior to those produced earlier in the design process.

Based on the data collected and the performance of other existing automated segmentation software, the algorithm created performs similar to existing software subject to the metrics the team evaluated. However, in order to get an accurate picture of how well it performs, the team's algorithm and the existing software should be tested and evaluated using the same data set. It is likely that the algorithm made will only work for the data set it was tested on. Therefore, further work and testing will need to be conducted in order to make the algorithm more robust.

Throughout the design of the solution, all decisions made were justified by stakeholders needs, as well as social, ethical, environmental, and economic impacts. Throughout the design process, the output of the algorithm was assessed based on its similarity to the ground truth produced by the medical professional. The metric used to assess the design was chosen so that the results of the design were as close to the standards set out by medical professionals as possible, for the good of all stakeholders.

Through the development of the project, the team learned that medical problems are often complicated, nuanced, and vary greatly from patient to patient. A general solution to a broad problem is rarely feasible and can result in a design that does not meet the desired specifications. When dealing with complex problems, the scope should be refined to a specific problem as soon as possible. Once the design meets the required criteria on the narrow problem, the scope can be expanded and the design can be gradually and iteratively improved to meet the new specifications. In the case of this project, the team should have focused on a specific type of lesion before expanding the scope to include a variety of different types.

For this project, the team attempted to automatically trace each lesion in an MRI file using only one given ground truth. This scope was well beyond the current state of the field. A more appropriate scope would have been to design an algorithm and a system that could trace the lesions with the ground truth of alternating layers given as input. When a design was created for this problem that met the required metrics, the scope could be expanded and the design iteratively improved upon.

Appendix

	file	Max Area	Min Area	Avg Delta Area	Max Delta Area	Min Delta Area	Avg Delta/Max Area	Max Delta/Max Area
0	c0001s0004t01.nii.gz	73	5	9.615384615	26	1	13.17%	35.62%
1	c0001s0005t01.nii.gz	432	9	29.75	105	1	6.89%	24.31%
2	c0001s0006t01.nii.gz	636	21	113.7272727	441	3	17.88%	69.34%
3	c0001s0007t01.nii.gz	1939	74	111.2615385	774	1	5.74%	39.92%
4	c0001s0008t01.nii.gz	1678	4	55.5942029	163	3	3.31%	9.71%
5	c0001s0012t01.nii.gz	2227	36	79.17283951	308	0	3.56%	13.83%
6	c0002s0001t01.nii.gz	438	22	24.48837209	129	0	5.59%	29.45%
7	c0002s0002t01.nii.gz	352	4	32.08333333	240	2	9.11%	68.18%
8	c0002s0003t01.nii.gz	356	29	23.67391304	71	1	6.65%	19.94%
9	c0002s0004t01.nii.gz	171	2	16.89473684	54	1	9.88%	31.58%
10	c0002s0005t01.nii.gz	217	34	33.25925926	89	1	15.33%	41.01%
11	c0002s0007t01.nii.gz	1152	7	63.171875	290	0	5.48%	25.17%
12	c0002s0008t01.nii.gz	423	6	25.43478261	87	2	6.01%	20.57%
13	c0002s0009t01.nii.gz	1139	1	64.13888889	354	1	5.63%	31.08%
14	c0002s0011t01.nii.gz	1751	29	104.5111111	454	2	5.97%	25.93%
15	c0002s0012t01.nii.gz	1439	4	49.65	139	3	3.45%	9.66%
16	c0002s0013t01.nii.gz	1725	4	126.5365854	629	2	7.34%	36.46%
17	c0002s0014t01.nii.gz	15	10	6.666666667	12	3	44.44%	80.00%
18	c0002s0015t01.nii.gz	677	6	59.26666667	281	0	8.75%	41.51%
19	c0002s0016t01.nii.gz	46	10	16.4	25	10	35.65%	54.35%
20	c0002s0017t01.nii.gz	217	87	33.18181818	98	7	15.29%	45.16%
21	c0002s0018t01.nii.gz	435	7	28.35714286	74	2	6.52%	17.01%
22	c0002s0019t01.nii.gz	1503	23	60.98529412	318	2	4.06%	21.16%
23	c0002s0020t01.nii.gz	103	21	29.88888889	57	3	29.02%	55.34%
24	c0002s0021t01.nii.gz	668	9	57.96	182	3	8.68%	27.25%
25	c0002s0022t01.nii.gz	163	13	18.47368421	60	1	11.33%	36.81%
26	c0002s0023t01.nii.gz	177	19	42.1	93	8	23.79%	52.54%
27	c0002s0024t01.nii.gz	172	7	19.10526316	35	7	11.11%	20.35%
28	c0002s0025t01.nii.gz	707	9	45.175	121	1	6.39%	17.11%
29	c0002s0026t01.nii.gz	87	10	18.22222222	35	2	20.95%	40.23%
30	c0002s0027t01.nii.gz	33	3	5.72	13	0	17.33%	39.39%
31	c0003s0001t01.nii.gz	202	11	38.7	86	11	19.16%	42.57%
32	c0003s0002t01.nii.gz	236	10	36.91666667	75	8	15.64%	31.78%
33	c0003s0003t01.nii.gz	22	6	3.8	10	0	17.27%	45.45%
34	c0003s0004t01.nii.gz	377	3	44.3125	148	2	11.75%	39.26%
35	c0003s0005t01.nii.gz	302	2	28.95238095	80	3	9.59%	26.49%
36	c0003s0006t01.nii.gz	4	3	1.666666667	3	1	41.67%	75.00%
37	c0003s0007t01.nii.gz	601	4	78.5	257	14	13.06%	42.76%
38	c0003s0008t01.nii.gz	11	2	2.857142857	5	1	25.97%	45.45%
39	c0003s0009t01.nii.gz	136	4	19.33333333	55	4	14.22%	40.44%
40	c0003s0010t01.nii.gz	307	1	35.23529412	81	1	11.48%	26.38%

	file	Max Area	Min Area	Avg Δ Area	Max Δ Area	Min Δ Area	Avg Δ/Max Area	Max Δ/Max Area
41	c0003s0011t01.nii.gz	71	7	11.46153846	28	2	16.14%	39.44%
42	c0003s0012t01.nii.gz	86	2	10	30	0	11.63%	34.88%
43	c0003s0013t01.nii.gz	148	2	20.92857143	76	2	14.14%	51.35%
44	c0003s0014t01.nii.gz	106	3	19	42	4	17.92%	39.62%
45	c0003s0015t01.nii.gz	217	2	30.85714286	73	6	14.22%	33.64%
46	c0003s0016t01.nii.gz	33	3	9	28	1	27.27%	84.85%
47	c0003s0017t01.nii.gz	66	11	17	49	6	25.76%	74.24%
48	c0003s0018t01.nii.gz	138	6	18.23529412	53	2	13.21%	38.41%
49	c0003s0019t01.nii.gz	208	6	23.27777778	64	1	11.19%	30.77%
50	c0003s0020t01.nii.gz	157	2	16.22222222	58	1	10.33%	36.94%
51	c0003s0021t01.nii.gz	15	6	4	8	1	26.67%	53.33%
52	c0003s0022t01.nii.gz	11	1	3	6	1	27.27%	54.55%
53	c0003s0023t01.nii.gz	34	1	6.7	14	0	19.71%	41.18%
54	c0003s0024t01.nii.gz	437	3	48.16666667	99	3	11.02%	22.65%
55	c0003s0025t01.nii.gz	377	1	45.82352941	130	1	12.15%	34.48%
56	c0003s0026t01.nii.gz	59	4	10.46153846	24	1	17.73%	40.68%
57	c0003s0027t01.nii.gz	113	6	18.33333333	47	2	16.22%	41.59%
58	c0003s0028t01.nii.gz	23	7	9.75	17	4	42.39%	73.91%
59	c0003s0029t01.nii.gz	111	8	18.16666667	52	1	16.37%	46.85%
60	c0003s0030t01.nii.gz	72	5	9.266666667	26	2	12.87%	36.11%
61	c0003s0031t01.nii.gz	422	15	53.26666667	140	9	12.62%	33.18%
62	c0003s0032t01.nii.gz	565	4	51.18181818	198	7	9.06%	35.04%
63	c0003s0033t01.nii.gz	82	20	19	40	3	23.17%	48.78%
64	c0003s0034t01.nii.gz	694	1	55.48	149	0	7.99%	21.47%
65	c0003s0035t01.nii.gz	191	2	26.21428571	68	2	13.72%	35.60%
66	c0003s0036t01.nii.gz	371	19	42.52941176	94	7	11.46%	25.34%
67	c0003s0037t01.nii.gz	119	12	24.8	47	2	20.84%	39.50%
68	c0003s0038t01.nii.gz	176	3	21.8125	77	4	12.39%	43.75%
69	c0003s0039t01.nii.gz	121	1	17.71428571	73	1	14.64%	60.33%
70	c0003s0040t01.nii.gz	73	10	13.58333333	29	0	18.61%	39.73%
71	c0003s0041t01.nii.gz	95	3	15.58333333	29	1	16.40%	30.53%
72	c0003s0042t01.nii.gz	190	10	31	77	1	16.32%	40.53%
73	c0003s0043t01.nii.gz	20	1	4.33333333	11	1	21.67%	55.00%
74	c0003s0044t01.nii.gz	156	9	27.54545455	82	6	17.66%	52.56%
75	c0003s0045t01.nii.gz	187	6	24.8	70	2	13.26%	37.43%
76	c0003s0046t01.nii.gz	30	3	5.090909091	10	2	16.97%	33.33%
77	c0003s0048t01.nii.gz	57	1	8.75	16	1	15.35%	28.07%
78	c0003s0049t01.nii.gz	23	1	6.333333333	14	1	27.54%	60.87%
79	c0003s0050t01.nii.gz	21	2	4.272727273	15	0	20.35%	71.43%
80	c0003s0051t01.nii.gz	102	2	20	47	0	19.61%	46.08%
81	c0003s0052t01.nii.gz	141	2	24.81818182	61	2	17.60%	43.26%
82	c0003s0053t01.nii.gz	74	5	10.46153846	33	0	14.14%	44.59%
83	c0003s0054t01.nii.gz	892	2	81	263	2	9.08%	29.48%
84	c0003s0055t01.nii.gz	35	9	12.2	18	3	34.86%	51.43%
85	c0003s0056t01.nii.gz	35	5	6.083333333	15	0	17.38%	42.86%

	file	Max Area	Min Area	Avg Δ Area	Max Δ Area	Min Δ Area	Avg Δ/Max Area	Max Δ/Max Area
86	c0004s0001t01.nii.gz	2266	8	58.85714286	116	1	2.60%	5.12%
87	c0004s0002t01.nii.gz	2771	2	73.74025974	222	0	2.66%	8.01%
88	c0004s0003t01.nii.gz	82	1	9.176470588	27	0	11.19%	32.93%
89	c0004s0004t01.nii.gz	874	1	45.425	180	1	5.20%	20.59%
90	c0004s0005t01.nii.gz	982	17	39.42592593	113	2	4.01%	11.51%
91	c0004s0006t01.nii.gz	55	16	18.8	31	1	34.18%	56.36%
92	c0004s0007t01.nii.gz	160	9	12.24324324	43	0	7.65%	26.88%
93	c0004s0008t01.nii.gz	74	1	10.21428571	35	1	13.80%	47.30%
94	c0004s0009t01.nii.gz	246	2	15.11627907	39	0	6.14%	15.85%
95	c0004s0010t01.nii.gz	1858	5	44.25	178	1	2.38%	9.58%
96	c0004s0011t01.nii.gz	459	3	29.41025641	81	4	6.41%	17.65%
97	c0004s0012t01.nii.gz	488	2	21.75	89	1	4.46%	18.24%
98	c0004s0013t01.nii.gz	268	1	16.61764706	38	1	6.20%	14.18%
99	c0004s0014t01.nii.gz	650	2	30.48888889	173	1	4.69%	26.62%
100	c0004s0015t01.nii.gz	264	1	14.07317073	60	0	5.33%	22.73%
101	c0004s0016t01.nii.gz	250	9	16.36666667	32	4	6.55%	12.80%
102	c0004s0017t01.nii.gz	42	2	7.25	16	0	17.26%	38.10%
103	c0004s0018t01.nii.gz	46	2	8.555555556	21	2	18.60%	45.65%
104	c0004s0019t01.nii.gz	1141	32	33.49350649	141	0	2.94%	12.36%
105	c0004s0020t01.nii.gz	1168	12	40.8630137	151	2	3.50%	12.93%
106	c0004s0021t01.nii.gz	143	4	10.23684211	42	0	7.16%	29.37%
107	c0004s0022t01.nii.gz	1755	3	58.7704918	154	3	3.35%	8.77%
108	c0004s0023t01.nii.gz	6	2	2.666666667	4	2	44.44%	66.67%
109	c0004s0024t01.nii.gz	78	2	11	33	2	14.10%	42.31%
110	c0004s0025t01.nii.gz	133	6	9.151515152	51	0	6.88%	38.35%
111	c0004s0026t01.nii.gz	202	13	20.57894737	101	1	10.19%	50.00%
112	c0004s0027t01.nii.gz	65	2	5.8	28	0	8.92%	43.08%
113	c0004s0028t01.nii.gz	42	20	16	22	7	38.10%	52.38%
114	c0004s0029t01.nii.gz	97	3	5.12244898	27	0	5.28%	27.84%
115	c0004s0030t01.nii.gz	228	5	11.0877193	56	0	4.86%	24.56%
116	c0004s0031t01.nii.gz	1228	5	43.875	124	1	3.57%	10.10%
117	c0004s0032t01.nii.gz	226	1	15	62	1	6.64%	27.43%
118	c0004s0033t01.nii.gz	824	10	25.46031746	67	2	3.09%	8.13%
119	c0004s0034t01.nii.gz	186	4	16.08695652	60	1	8.65%	32.26%
120	c0005s0003t01.nii.gz	330	6	24.46153846	66	3	7.41%	20.00%
121	c0005s0006t01.nii.gz	122	14	8.068965517	30	0	6.61%	24.59%
122	c0005s0007t01.nii.gz	1659	9	47.15277778	159	1	2.84%	9.58%
123	c0005s0008t01.nii.gz	73	9	6.214285714	22	0	8.51%	30.14%
124	c0005s0009t01.nii.gz	923	6	32.24137931	82	1	3.49%	8.88%
125	c0005s0010t01.nii.gz	24	2	4.222222222	12	1	17.59%	50.00%
126	c0005s0011t01.nii.gz	276	3	15.09756098	48	1	5.47%	17.39%
127	c0005s0012t01.nii.gz	191	2	25.333333333	54	1	13.26%	28.27%
128	c0005s0013t01.nii.gz	2041	5	51.14457831	254	0	2.51%	12.44%
129	c0005s0014t01.nii.gz	823	1	31.26415094	90	1	3.80%	10.94%
130	c0005s0017t01.nii.gz	840	3	30.41071429	86	0	3.62%	10.24%

	file	Max Area	Min Area	Avg Δ Area	Max Δ Area	Min Δ Area	Avg Δ/Max Area	Max Δ/Max Area
131	c0005s0018t01.nii.gz	327	1	18.65714286	50	0	5.71%	15.29%
132	c0005s0021t01.nii.gz	40	7	12.4	22	4	31.00%	55.00%
133	c0005s0024t01.nii.gz	13	5	4.2	7	1	32.31%	53.85%
134	c0005s0026t01.nii.gz	405	6	25.09375	119	0	6.20%	29.38%
135	c0005s0027t01.nii.gz	25	1	3.636363636	12	0	14.55%	48.00%
136	c0005s0028t01.nii.gz	20	3	7.4	10	3	37.00%	50.00%
137	c0005s0029t01.nii.gz	245	14	15.5	60	0	6.33%	24.49%
138	c0005s0030t01.nii.gz	2688	3	63.13953488	227	1	2.35%	8.44%
139	c0005s0031t01.nii.gz	59	1	12.66666667	22	1	21.47%	37.29%
140	c0005s0035t01.nii.gz	285	2	15.14893617	37	0	5.32%	12.98%
141	c0005s0036t01.nii.gz	1600	2	38.37647059	163	0	2.40%	10.19%
142	c0005s0040t01.nii.gz	8	4	4	8	0	50.00%	100.00%
143	c0005s0042t01.nii.gz	168	3	10.59375	28	0	6.31%	16.67%
144	c0005s0043t01.nii.gz	1005	1	34.18181818	110	0	3.40%	10.95%
145	c0005s0044t01.nii.gz	24	8	5.142857143	14	0	21.43%	58.33%
146	c0005s0045t01.nii.gz	107	6	19.7	69	1	18.41%	64.49%
147	c0005s0047t01.nii.gz	34	5	7.076923077	14	3	20.81%	41.18%
148	c0005s0048t01.nii.gz	25	1	9	17	1	36.00%	68.00%
149	c0005s0049t01.nii.gz	45	1	4.16	11	1	9.24%	24.44%
Average							13.85%	35.49%
Variance							1.02%	3.30%

	file	Avg X	Avg Y	Max Distance	Min Distance	Avg Distance
0	c0001s0004t01.nii.gz	144.1417605	141.8875673	1.086055643	0.323634078	0.572878661
1	c0001s0005t01.nii.gz	103.8343884	150.3587508	3.694564692	0.169538526	1.378148792
2	c0001s0006t01.nii.gz	173.4557433	173.6103899	3.944439696	0.99128539	2.521458907
3	c0001s0007t01.nii.gz	85.09213539	144.8511345	14.82176041	0.253997173	2.620329557
4	c0001s0008t01.nii.gz	98.82685124	143.1391648	9.38595829	0.065524079	1.204798553
5	c0001s0012t01.nii.gz	147.5941359	169.7819653	7.102126246	0.142877793	1.277452621
6	c0002s0001t01.nii.gz	101.6847661	138.8885212	4.299420787	0.23087736	1.031140931
7	c0002s0002t01.nii.gz	154.8053918	139.3450638	11.17554459	0.142568826	1.53370924
8	c0002s0003t01.nii.gz	109.6751724	156.6884575	3.402522623	0.005622039	1.145128495
9	c0002s0004t01.nii.gz	104.6530703	136.0020899	2.444114593	0.25442846	1.163613149
10	c0002s0005t01.nii.gz	159.3924474	153.6351624	7.026728003	0.366936322	2.057911863
11	c0002s0007t01.nii.gz	90.0444727	149.8514553	6.849081405	0.04744372	1.7344708
12	c0002s0008t01.nii.gz	104.012318	149.6532343	3.071137045	0.210406648	1.078591481
13	c0002s0009t01.nii.gz	77.90495299	137.1748083	4.703401626	0.351303571	1.545900042
14	c0002s0011t01.nii.gz	85.4114813	155.0504857	11.10241648	0.22595853	2.051024544
15	c0002s0012t01.nii.gz	97.18908374	145.2789901	18.52258521	0.095038396	1.200565906
16	c0002s0013t01.nii.gz	79.28855798	168.4167507	25.36692598	0.260501115	3.369105039
17	c0002s0014t01.nii.gz	151.9666667	123.5722222	0.405517502	0.393347457	0.39943248
18	c0002s0015t01.nii.gz	106.2305511	170.6821867	10.41914099	0.08642406	2.136648805
19	c0002s0016t01.nii.gz	129.8341163	106.6939469	2.879377767	0.323175408	1.750592982
20	c0002s0017t01.nii.gz	105.8193364	168.8092782	5.648449061	0.300810945	2.0180992
21	c0002s0018t01.nii.gz	161.7675707	144.7636324	7.427371836	0.225876976	1.800106411
22	c0002s0019t01.nii.gz	176.8213489	128.573037	3.69080126	0.081138529	1.00672534
23	c0002s0020t01.nii.gz	99.68425604	132.8839892	4.635125524	0.508380414	2.31155455
24	c0002s0021t01.nii.gz	161.4384512	144.5791593	5.234041636	0.230497181	1.966570611
25	c0002s0022t01.nii.gz	152.9493212	145.6289572	4.307658801	0.134007686	1.381597505
26	c0002s0023t01.nii.gz	124.8005403	96.30983062	2.014601774	0.504471683	1.25411178
27	c0002s0024t01.nii.gz	148.8225099	142.4546303	3.970413557	0.223820806	1.125398957
28	c0002s0025t01.nii.gz	92.4788856	137.8000854	9.227300445	0.055025251	1.469182255
29	c0002s0026t01.nii.gz	126.3197412	98.34039359	2.773629494	0.182859377	1.01385354
30	c0002s0027t01.nii.gz	113.5439737	154.6988752	2.866279044	0.177272727	1.034411947
31	c0003s0001t01.nii.gz	131.4915938	155.3920177	2.866881278	0.352374258	1.271406547
32	c0003s0002t01.nii.gz	137.0688541	155.5356083	2.679240845	0.271964183	1.247496604
33	c0003s0003t01.nii.gz	139.2418983	148.2358974	0.359517052	0	0.172204991
34	c0003s0004t01.nii.gz	138.6117285	157.8231279	7.586356174	0.213079288	2.090986408
35	c0003s0005t01.nii.gz	139.5102364	140.8880325	4.146131924	0.162549841	1.390024634
36	c0003s0006t01.nii.gz	144.2777778	152.6111111	0.849836586	0.23570226	0.542769423
37	c0003s0007t01.nii.gz	123.3153697	139.8271783	6.457406319	0.953864788	2.607492226
38	c0003s0008t01.nii.gz	143.2111781	136.0349722	0.895134345	0.279508497	0.492473857
39	c0003s0009t01.nii.gz	126.2202485	131.1363769	1.654462117	0.353116635	1.068208412
40	c0003s0010t01.nii.gz	156.2952578	151.146285	7.163650331	0.418808997	1.469955165

	file	Avg X	Avg Y	Max Distance	Min Distance	Avg Distance
41	c0003s0011t01.nii.gz	122.946816	121.6476571	5.117199279	0.445109467	1.873079315
42	c0003s0012t01.nii.gz	125.0778073	165.3624243	1.258228337	0.185776833	0.622259243
43	c0003s0013t01.nii.gz	139.8603924	146.11961	3.535898117	0.214285714	1.663668109
44	c0003s0014t01.nii.gz	133.4402982	171.2100964	3.721674918	0.641480923	1.846537996
45	c0003s0015t01.nii.gz	143.0432407	165.029894	4.972750586	0.15621142	1.259622501
46	c0003s0016t01.nii.gz	129.9492284	138.0577005	2.955562817	0.051807119	1.140886001
47	c0003s0017t01.nii.gz	124.1206978	154.6690234	2.837043835	0.628017044	1.600198941
48	c0003s0018t01.nii.gz	126.5173393	160.0011336	10.01281858	0.291875802	2.08800942
49	c0003s0019t01.nii.gz	131.679714	174.4311328	5.65933349	0.363859285	2.034396488
50	c0003s0020t01.nii.gz	123.8523061	171.8797992	1.025501288	0.163888694	0.587745306
51	c0003s0021t01.nii.gz	143.9956349	150.8833333	0.533593686	0.28096247	0.373143126
52	c0003s0022t01.nii.gz	137.5639971	158.8829966	0.697262418	0.285714286	0.467504449
53	c0003s0023t01.nii.gz	136.4952206	159.5967415	43.91556137	0	6.065359468
54	c0003s0024t01.nii.gz	114.7747787	144.3910537	7.189146974	0.23570226	2.135844209
55	c0003s0025t01.nii.gz	140.1663415	156.1476551	10.37575298	0.291335738	1.890638836
56	c0003s0026t01.nii.gz	142.4174902	145.454666	2.418373613	0.321536826	1.478906845
57	c0003s0027t01.nii.gz	123.958408	168.2749414	1.737494806	0.225322464	0.700976042
58	c0003s0028t01.nii.gz	136.4403977	150.6800185	0.63610925	0.095563446	0.289073245
59	c0003s0029t01.nii.gz	127.966687	153.7436965	6.343638281	0.076385197	2.384817238
60	c0003s0030t01.nii.gz	98.78328952	188.3495066	2.55867878	0.159352451	0.669630145
61	c0003s0031t01.nii.gz	120.6165434	161.361263	3.191696599	0.147760291	1.000488974
62	c0003s0032t01.nii.gz	133.0311532	181.0364863	9.132871215	0.096712461	1.33445205
63	c0003s0033t01.nii.gz	128.1681408	174.2073622	0.805985067	0.156569119	0.553041113
64	c0003s0034t01.nii.gz	130.0373123	152.8776259	48.75705077	0	3.736904929
65	c0003s0035t01.nii.gz	142.8375193	177.9003435	7.406669617	0.65329176	2.183044777
66	c0003s0036t01.nii.gz	122.5517005	179.0952073	3.604077518	0.1792306	1.45292074
67	c0003s0037t01.nii.gz	111.6564127	171.1875299	4.750982278	0.642780516	2.56266841
68	c0003s0038t01.nii.gz	139.1518801	184.6527	3.421275306	0.225311137	1.111973269
69	c0003s0039t01.nii.gz	135.5599236	173.5944046	6.577141036	0.291161616	1.977546834
70	c0003s0040t01.nii.gz	142.461774	178.4108567	4.959205152	0.48926049	1.625517551
71	c0003s0041t01.nii.gz	126.9960547	178.6419299	6.595318787	0.404917204	2.022990702
72	c0003s0042t01.nii.gz	127.5405209	159.8818428	5.892828033	0.547747018	2.049404161
73	c0003s0043t01.nii.gz	135.865812	181.9444057	1.532064693	0.296153088	0.660879246
74	c0003s0044t01.nii.gz	128.6451601	155.236303	5.616567568	0.517379785	1.745911731
75	c0003s0045t01.nii.gz	131.6030752	179.647242	3.048630227	0.185763884	1.382315477
76	c0003s0046t01.nii.gz	132.7070249	165.9759491	1.008060588	0.188561808	0.545724465
77	c0003s0048t01.nii.gz	136.3245808	166.3205179	5.852349955	0.155226271	1.378303508
78	c0003s0049t01.nii.gz	128.7839903	176.438909	3.966548493	0.395284708	1.610810815
79	c0003s0050t01.nii.gz	104.7318772	151.6023219	3.301178241	0.19047619	0.935924932
80	c0003s0051t01.nii.gz	127.6867617	175.5556511	8.373735675	0.376087851	2.63584369

	file	Avg X	Avg Y	Max Distance	Min Distance	Avg Distance
81	c0003s0052t01.nii.gz	126.4193662	153.8728283	3.924615435	0.424910954	1.555988794
82	c0003s0053t01.nii.gz	128.0822402	180.9263438	1.351725007	0.164953454	0.700731433
83	c0003s0054t01.nii.gz	108.9110954	164.2011009	7.991873403	0.327184116	2.287333456
84	c0003s0055t01.nii.gz	131.6101579	155.1702338	1.807576866	0.629859931	1.231533885
85	c0003s0056t01.nii.gz	143.0974584	179.7003246	2.85465568	0.233432202	1.355112815
86	c0004s0001t01.nii.gz	129.0411924	123.0139561	2.880014497	0.012899913	0.750262046
87	c0004s0002t01.nii.gz	135.4424158	106.1559909	8.866396638	0.057163465	1.475533639
88	c0004s0003t01.nii.gz	105.9369099	111.6701421	2.511921688	0.214285714	0.913480429
89	c0004s0004t01.nii.gz	54.44332574	88.07490317	2.213656931	0.04128356	0.79122626
90	c0004s0005t01.nii.gz	55.993984	106.6126981	9.940091417	0.10314666	1.758043426
91	c0004s0006t01.nii.gz	88.37190443	97.67108828	1.308841908	0.722582144	0.920274597
92	c0004s0007t01.nii.gz	109.8307203	110.0626502	4.793029349	0.091624569	1.114773485
93	c0004s0008t01.nii.gz	79.29264128	97.93887579	50.44799302	0.311840679	9.825429179
94	c0004s0009t01.nii.gz	121.9947742	76.93808653	13.67916413	0.062791847	1.686220864
95	c0004s0010t01.nii.gz	131.4831495	89.43111085	2.711536929	0.029836694	0.855848165
96	c0004s0011t01.nii.gz	112.5562583	94.52605764	4.527692569	0.099317844	1.252547887
97	c0004s0012t01.nii.gz	58.39124799	84.45314989	4.51506395	0.146934193	1.158612991
98	c0004s0013t01.nii.gz	58.27207593	93.51520751	1.717239397	0.017987513	0.581730275
99	c0004s0014t01.nii.gz	61.80653751	89.72656465	12.69290369	0.077918901	2.133921464
100	c0004s0015t01.nii.gz	65.26392226	95.84446695	2.388139417	0.014444296	0.626307494
101	c0004s0016t01.nii.gz	51.29560364	103.1673211	2.159217965	0.06177469	0.673252658
102	c0004s0017t01.nii.gz	94.08141608	77.01429999	3.157130139	0.240551475	1.135188888
103	c0004s0018t01.nii.gz	61.60311438	118.9366626	1.769573081	0.275939509	0.84052211
104	c0004s0019t01.nii.gz	111.7376964	99.73249384	2.533583111	0.079965525	0.915416437
105	c0004s0020t01.nii.gz	126.60508	114.8113443	14.37914315	0.097466821	1.138236406
106	c0004s0021t01.nii.gz	98.97182903	92.79101756	60.49876032	0.098666062	2.587346935
107	c0004s0022t01.nii.gz	62.05404218	107.8001185	11.09275263	0.097786357	1.458555764
108	c0004s0023t01.nii.gz	80.72222222	103.5	0.333333333	0.166666667	0.25
109	c0004s0024t01.nii.gz	86.336366	119.9442634	3.362509645	0.347858881	1.243438421
110	c0004s0025t01.nii.gz	102.3045739	103.0911977	4.913443229	0.031765412	0.51556391
111	c0004s0026t01.nii.gz	55.58777818	107.3315393	2.357595631	0.156656036	0.715052643
112	c0004s0027t01.nii.gz	59.5987094	104.315846	2.132930631	0.194222356	0.779820344
113	c0004s0028t01.nii.gz	95.71845238	93.1077381	0.876843701	0.08151068	0.451760451
114	c0004s0029t01.nii.gz	57.81119845	96.91979256	2.402140207	0.184966944	0.669185647
115	c0004s0030t01.nii.gz	53.52924135	73.12892442	3.284516673	0.038897529	0.854932599
116	c0004s0031t01.nii.gz	50.7713397	97.45644991	4.362728287	0.065391461	0.924331294
117	c0004s0032t01.nii.gz	69.32162134	103.9662165	3.127847487	0.118419291	0.851208776
118	c0004s0033t01.nii.gz	49.36228157	111.3786104	4.080630779	0.056186128	0.824954825
119	c0004s0034t01.nii.gz	51.86730322	81.43517605	3.623150416	0.397510562	1.133369969
120	c0005s0003t01.nii.gz	97.3964104	110.576215	3.739193629	0.035015876	0.709037533

	file	Avg X	Avg Y	Max Distance	Min Distance	Avg Distance
121	c0005s0006t01.nii.gz	100.2191499	91.34697514	1.632841457	0.10249628	0.73259123
122	c0005s0007t01.nii.gz	91.4706219	109.2891658	3.552704874	0.068862586	0.832825656
123	c0005s0008t01.nii.gz	106.6389966	101.3992711	2.356459203	0.077736652	0.662782287
124	c0005s0009t01.nii.gz	99.22563796	106.9060112	5.713733697	0.094073069	1.291110696
125	c0005s0010t01.nii.gz	115.3453944	111.9548341	0.891650897	0.098169182	0.50880972
126	c0005s0011t01.nii.gz	105.9428931	79.07766608	5.656265666	0.090887956	1.757390037
127	c0005s0012t01.nii.gz	155.0691686	58.46838782	4.235540128	0.589623821	2.455294023
128	c0005s0013t01.nii.gz	113.8892774	125.068868	4.954140894	0.027386681	1.126373492
129	c0005s0014t01.nii.gz	106.1256316	102.9277013	3.302539637	0.209010886	0.795952069
130	c0005s0017t01.nii.gz	96.28511037	107.3830442	10.9825609	0.066705487	1.661593052
131	c0005s0018t01.nii.gz	100.759978	96.69838789	5.887553556	0.08873921	1.077267449
132	c0005s0021t01.nii.gz	162.6374357	82.62450192	1.628822036	0.424918293	0.888508538
133	c0005s0024t01.nii.gz	105.1782051	50.91683761	0.783510618	0.387265325	0.498495943
134	c0005s0026t01.nii.gz	103.9680249	95.86437926	6.887680964	0.032258065	1.438731475
135	c0005s0027t01.nii.gz	144.3710361	94.60557272	82.57933895	0.198528286	8.71742005
136	c0005s0028t01.nii.gz	163.1604374	53.68608346	1.590317263	0.746677937	0.984257548
137	c0005s0029t01.nii.gz	102.6070867	81.24880959	2.958753891	0.119889028	0.634145953
138	c0005s0030t01.nii.gz	114.0719456	125.2294667	6.184814403	0.071785014	1.249552612
139	c0005s0031t01.nii.gz	134.0686338	86.76421092	3.597066706	0	1.246692876
140	c0005s0035t01.nii.gz	103.3029621	96.45725749	1.827921629	0.116210542	0.870676229
141	c0005s0036t01.nii.gz	88.18030736	114.312648	6.562206933	0.138256064	0.796794672
142	c0005s0040t01.nii.gz	118.375	96.04166667	0.728868987	0.530330086	0.629599536
143	c0005s0042t01.nii.gz	98.45233132	69.29828128	2.021382955	0.109286715	0.893086426
144	c0005s0043t01.nii.gz	96.18282587	115.7434871	11.6831179	0	1.311595398
145	c0005s0044t01.nii.gz	109.0107143	86.93971861	1.019059078	0.093169499	0.319284466
146	c0005s0045t01.nii.gz	123.1395814	88.30947945	0.886764437	0.184934647	0.50278135
147	c0005s0047t01.nii.gz	96.61684912	64.94084326	2.125918919	0.256436263	1.13938783
148	c0005s0048t01.nii.gz	122.6414545	85.33672727	2.904897546	0.5	1.712474355
149	c0005s0049t01.nii.gz	95.50458758	99.27378605	2.963485873	0.186338998	1.008658425

	file	Max Intensity	Min Intensity	Average Intensity	Max Δ Intensity	Min Δ Intensity	Average Δ Intensity	Max Variance	Min Variance
0	c0001s0004t01.nii.gz	56	36.55319149	43.96046755	10.35483871	0.270001985	4.028010357	231.9322773	32.8
1	c0001s0005t01.nii.gz	66.5505618	58.46478873	62.01591796	4.837728195	0.154010074	1.438558456	187.3191827	4.320987654
2	c0001s0006t01.nii.gz	34.73854962	21.76190476	28.59452378	7.70240504	0.353988108	2.024380932	140.8603204	54.93652344
3	c0001s0007t01.nii.gz	37.43103448	21.8364486	29.78141186	5.706930234	0.040793949	1.614846371	113.0439611	13.10731272
4	c0001s0008t01.nii.gz	50.38095238	33.28	41.19454844	10.863711	6.237241379	8.473650794	91.1616	23.09297052
5	c0001s0012t01.nii.gz	43.66359447	8.113207547	26.00111152	11.71236559	0.023876001	1.086650147	122.3775404	19.78980229
6	c0002s0001t01.nii.gz	61.81818182	44.07294118	52.60722557	4.570909091	0.095996732	1.317900777	186.4685727	8.0416
7	c0002s0002t01.nii.gz	72.1	59.84146341	64.03592659	4.637037037	0.102346041	1.050840018	66.16102041	3.29
8	c0002s0003t01.nii.gz	65.17460317	52.1322314	58.24242704	3.334375	0.024198167	1.196594426	144.0984854	10.17360285
9	c0002s0004t01.nii.gz	51	32	43.50098475	7.693181818	0.062847094	1.905733422	112.8774196	1
10	c0002s0005t01.nii.gz	70.93719807	51.27586207	65.09498425	8.213511259	0.002439024	2.663851888	257.6285121	17.20888889
11	c0002s0007t01.nii.gz	66.84745763	41.14485981	59.12932451	7.705404061	0.025016118	1.076149341	166.9969463	11.14622235
12	c0002s0008t01.nii.gz	69.58823529	54.35064935	61.32862985	8.012477718	0.162597403	1.464346449	180.9905146	8.805555556
13	c0002s0009t01.nii.gz	35.80508475	20	28.72245529	6.162162162	0.031402742	1.404650727	132.8647305	0
14	c0002s0011t01.nii.gz	38.48987854	27.04651163	32.62163014	6.275838373	0.094647717	1.385108581	182.4332072	10.92042517
15	c0002s0012t01.nii.gz	33.4	17.66037736	23.56406538	14.08962264	0.007700914	0.853206029	151.6875	6.24
16	c0002s0013t01.nii.gz	35.07525326	18.625	26.13209337	6.256952719	0.058776178	2.087952935	249.2475931	3.666666667
17	c0002s0014t01.nii.gz	46.7	44.06666667	45.36666667	2.633333333	1.266666667	1.95	189.1288889	109.81
18	c0002s0015t01.nii.gz	54.82191781	23.16666667	44.59045925	12.13709677	0.187878788	1.984761018	180.8521722	6.472222222
19	c0002s0016t01.nii.gz	48.5	34.23809524	43.38560888	13.21645022	1.778881988	6.869588745	203.0756144	14.45
20	c0002s0017t01.nii.gz	45.64705882	25.95555556	33.18494081	8.386001029	0.234294872	2.880013287	177.6245891	22.69896194
21	c0002s0018t01.nii.gz	53.84337349	31.77777778	37.96843645	7.521231751	0.030701754	1.969060933	332.8163265	39.63811874
22	c0002s0019t01.nii.gz	40.2173913	24.85940594	30.65790629	5.028712059	0.04423816	0.862598144	122.1757354	21.40959895
23	c0002s0020t01.nii.gz	48.3	30.86440678	40.79082475	8.7898435	1.769992384	5.853569357	210.4513146	50.1172077
24	c0002s0021t01.nii.gz	52.4	28.22222222	38.96458782	8.54320031	0.460818713	3.13406082	223.8552105	41.63459459
25	c0002s0022t01.nii.gz	59.33333333	37.61111111	46.22531773	9.081196581	0.391538102	4.037757314	180.782872	18.6984127
26	c0002s0023t01.nii.gz	49.88888889	38.8852459	44.29032333	7.236803874	2.335093081	5.143884986	94.7573233	10.87654321
27	c0002s0024t01.nii.gz	48.125	33	40.09965533	8.714285714	0.396101019	3.87093591	163.4419216	0
28	c0002s0025t01.nii.gz	55.66666667	46.07692308	49.54628011	8.541666667	0.215909091	3.002564103	69.17355372	2.888888889
29	c0002s0026t01.nii.gz	49.75	44.47142857	46.45615614	4.161764706	0.277618364	1.991910686	105.1920408	0.1875
30	c0002s0027t01.nii.gz	55.1	38.75	47.32329789	8.309090909	0.404166667	2.941578345	164.3888889	5.09
31	c0003s0001t01.nii.gz	2676	1541.775	1994.35042	543.5454545	31.7771261	250.025	305807.5148	81
32	c0003s0002t01.nii.gz	2323.333333	1841.634409	2102.439781	197.7838875	19.52136752	102.8843787	133666.1244	2921.333333
33	c0003s0003t01.nii.gz	2454.166667	1486.5	1710.533192	489.8541667	20.98529412	134.639518	440322.2493	71860.80556
34	c0003s0004t01.nii.gz	2646.08	1608.978648	2181.894784	474.8630973	5.75	144.4100002	446471.1659	8632.4375
35	c0003s0005t01.nii.gz	2691.333333	1424	2072.463328	465	5.07740448	108.6519182	440375.732	2601
36	c0003s0006t01.nii.gz	1965.666667	1926	1939.972222	37.41666667	2.25	19.833333333	115778.1875	67680.66667
37	c0003s0007t01.nii.gz	3107.5	2048.9046	2428.975102	323.5	6.779791617	126.2874248	427094.9284	18438.25
38	c0003s0008t01.nii.gz	2574.5	1836.142857	2196.511967	385.8571429	50.73214286	187.3690476	151768.3594	1296

	file	Max Intensity	Min Intensity	Average Intensity	Max Δ Intensity	Min Δ Intensity	Average Δ Intensity	Max Variance	Min Variance
39	c0003s0009t01.nii.gz	2496.071429	1717.2	2043.871295	329.636646	40.35714286	178.1119048	276126.4375	0
40	c0003s0010t01.nii.gz	2349	1651.666667	2054.597223	372.8843537	8.141608392	75.66248338	241976.3556	0
41	c0003s0011t01.nii.gz	2572.277778	2339.533333	2460.154202	126.6571429	1.620915033	68.28412698	111075.4691	14734.6875
42	c0003s0012t01.nii.gz	2306	2134.75	2200.407265	143.4444444	12.48076923	72	49264.1875	16805.25
43	c0003s0013t01.nii.gz	2160.479167	1858.708333	1990.725706	178.962069	16.31166667	80.77130952	121458.2866	14540.75667
44	c0003s0014t01.nii.gz	2488.2	1323.916667	1730.583388	412.6878049	39.31487117	175.7366667	584560.1901	26797.96
45	c0003s0015t01.nii.gz	1640.176471	1260.833333	1427.356961	262.1098039	57.625	144.0441176	205670.8889	65907.78993
46	c0003s0016t01.nii.gz	2437.5	1569.473684	1966.074225	344.8125	89.58333333	233.2865497	414543.0156	32864.66667
47	c0003s0017t01.nii.gz	2547	2103.142857	2317.661905	259.5	87	154.5952381	81649.08333	0
48	c0003s0018t01.nii.gz	2345.6	1764.32	2080.90411	427.906746	5.842604433	148.3118923	361704.4799	27755.04
49	c0003s0019t01.nii.gz	2780.333333	2041.626374	2375.654785	184.880907	3.225174216	73.28103418	394814.9521	1861.222222
50	c0003s0020t01.nii.gz	2635.045455	1796.654676	2057.221273	312.4865385	7.899895178	110.7468674	485977.8785	702.25
51	c0003s0021t01.nii.gz	1992	1479.125	1675.764881	227	8.702380952	123.075	206554.3112	45218
52	c0003s0022t01.nii.gz	2203.25	1433.142857	1841.994264	756.8571429	89.15714286	305.3928571	289013.6529	0
53	c0003s0023t01.nii.gz	2163.5	1328	1654.089319	329.0782609	20.72352941	172.4004669	410421.96	0
54	c0003s0024t01.nii.gz	2491.428571	2187.72973	2355.81673	135.4069264	27.61038961	86.10273028	192953.6875	12137.38776
55	c0003s0025t01.nii.gz	2226	1886.709677	2045.412692	175	41.10282258	101.9301075	131182.6316	0
56	c0003s0026t01.nii.gz	2866.5	1943.813559	2285.833394	515.3552632	18.91493268	167.1490016	428996.343	33161.58333
57	c0003s0027t01.nii.gz	2457	1885.352941	2165.729329	431.6153846	27.03167421	257.5735294	276542.0828	0
58	c0003s0028t01.nii.gz	2441.285714	1294.304348	1815.189311	782.7067669	364.2745995	573.088418	234208.5595	43111.06122
59	c0003s0029t01.nii.gz	2398.888889	1946.617647	2180.169281	202.2088484	0.302681992	101.1583369	358643.0205	8343.654321
60	c0003s0030t01.nii.gz	2619.4	2378.25	2499.320791	117.1691176	11.28982301	62.23519467	91520.84821	9865.84
61	c0003s0031t01.nii.gz	1472.2	1133.459459	1340.453368	221.7833333	6.880952381	66.55542296	65617.13889	9073.6875
62	c0003s0032t01.nii.gz	1276	891.75	1055.583333	384.25	107.25	245.75	54769.6875	0
63	c0003s0033t01.nii.gz	1748.354839	1159.48	1451.840065	371.3676471	27.52	194.7741398	110604.0156	22281.6875
64	c0003s0034t01.nii.gz	2177	1131.5	1717.086954	628	0.382341919	83.10460849	53715.54081	0
65	c0003s0035t01.nii.gz	2179.27551	1418.95	1740.290685	204.4126984	4.592583375	79.04436359	235737.1474	7850.216538
66	c0003s0036t01.nii.gz	1748.826087	1353.947368	1490.642356	130.4276316	1.556028761	36.56875017	179023.3492	48364.8828
67	c0003s0037t01.nii.gz	1014.732143	560.3333333	840.5233986	225.4591195	19.76805816	83.15042052	149541.4528	12045.05556
68	c0003s0038t01.nii.gz	1801.666667	1473.861111	1608.404348	217.7179487	23.01388889	95.46296296	105551.4427	6808
69	c0003s0039t01.nii.gz	1190.709677	836.5238095	957.5393674	354.1858679	8.860805861	181.5233369	94437.23829	34330.15976
70	c0003s0040t01.nii.gz	1735.230769	1222.6	1513.524074	207.5057692	46.46266234	101.437578	183011.9828	25552.84
71	c0003s0041t01.nii.gz	1767.666667	1303.428571	1581.854027	302.4081633	11.37505071	110.385777	143630.2571	3334.888889
72	c0003s0042t01.nii.gz	1386.1	756.4	1107.590943	231.4714286	1.446666667	131.8014956	138103.7636	12059.1875
73	c0003s0043t01.nii.gz	1116.4	849.6363636	956.6810366	160.6283422	0.786713287	89.18344988	77316.95868	24359.57333
74	c0003s0044t01.nii.gz	1479	1177.931034	1298.742775	118.1818182	25.58211144	73.96541275	70852.75386	484
75	c0003s0045t01.nii.gz	1647.782609	1243.293478	1490.257551	280.3731884	12.16485507	76.22114123	225948.7149	1804.666667
76	c0003s0046t01.nii.gz	1460	1264.125	1349.59024	195.875	1.273809524	71.32422071	83769.55102	15434
77	c0003s0048t01.nii.gz	1472.75	728.6	1021.640053	331.8088235	153.4	224.3875	101755.84	14203.6875
78	c0003s0049t01.nii.gz	1268	1034.2	1152.915521	167.925	6.25	58.41110013	75596.5625	0
79	c0003s0050t01.nii.gz	1363	719.4545455	956.2477076	324.125	8.845454545	181.3614719	93298.65	2116
80	c0003s0051t01.nii.gz	1243.878049	813	995.7411057	189.6917743	7.6288854	66.63091742	70841.71832	361

	file	Max Intensity	Min Intensity	Average Intensity	Max Δ Intensity	Min Δ Intensity	Average Δ Intensity	Max Variance	Min Variance
81	c0003s0052t01.nii.gz	1822.111111	1219.125	1447.090671	208.7037037	21.08122109	92.95010301	149325.8594	13302.76543
82	c0003s0053t01.nii.gz	1223.545455	894.2857143	987.3131494	329.2597403	1.6	81.79480519	47183.01653	1452.666667
83	c0003s0054t01.nii.gz	1677.529412	1277.657143	1503.713146	204.84	1.729411765	64.68267644	184250.4539	97
84	c0003s0055t01.nii.gz	1367.222222	1139.028571	1271.998045	142.9513889	84.90892857	114.0134921	48004.80859	10956.83951
85	c0003s0056t01.nii.gz	1342	995.3103448	1170.728763	187.2107143	6.72688172	82.05712609	143277.7041	7810.64
86	c0004s0001t01.nii.gz	1822	902	1443.571044	920	89.26262626	319.0872727	94864	0
87	c0004s0002t01.nii.gz	1797.875	1310.8	1562.215	370.6	37	214.41875	386249.5556	102823.04
88	c0004s0003t01.nii.gz	2590.9	1584.304348	2028.348221	672.0208333	29.73565217	303.1041063	337418.8204	19468.55556
89	c0004s0004t01.nii.gz	2224.379953	1398.604891	1705.759148	234.5263158	3.817894205	61.18107275	785340.372	0
90	c0004s0005t01.nii.gz	3215.510949	2475.522599	2962.825524	215.577027	0.016068784	53.45879259	514259.6606	23002.9161
91	c0004s0006t01.nii.gz	3280.923077	2163.542857	2553.750861	351.4108696	0.659465829	124.1241938	566988.1213	15790.22485
92	c0004s0007t01.nii.gz	2951.285714	2067.692308	2428.426054	378.6386555	67.48521739	169.8430141	168311.3163	970.6666667
93	c0004s0008t01.nii.gz	4958.441558	4046.285714	4504.228523	326.091043	6.944444444	168.1622579	1038510.415	22491.6875
94	c0004s0009t01.nii.gz	3458	1908.666667	2496.800285	519.6111111	3.265949821	195.2129403	600519.7941	31862.25
95	c0004s0010t01.nii.gz	2977.983834	1701.97416	2290.953636	356.9142857	0.824141309	56.77341916	1002432.981	149855.3469
96	c0004s0011t01.nii.gz	3353.333333	2682.666667	3086.392857	427.8333333	13.08333333	168.3472222	252764.8889	5929
97	c0004s0012t01.nii.gz	1901	1350	1625.5	551	551	551	91218.5	0
98	c0004s0013t01.nii.gz	2577.666667	1015.4	1724.623956	698.9636364	3.666769389	145.2394279	842140.2152	208733.1405
99	c0004s0014t01.nii.gz	3396.27027	2224.5	2888.918633	332.8333333	1.772486772	67.74735791	447777.9531	16277.78284
100	c0004s0015t01.nii.gz	2219	1741.7	1958.52963	477.3	173.1888889	325.2444444	384357.2099	21904
101	c0004s0016t01.nii.gz	3111	2554.625	2760.163462	544.8461538	73.38461538	221.1610577	361185.7344	148782.75
102	c0004s0017t01.nii.gz	2912.6	2267.771429	2417.118424	224.0100966	3.159041394	63.91272047	224876.4892	76354.04
103	c0004s0018t01.nii.gz	2246	1398.166667	1614.239278	429.1666667	2.313823857	189.9746212	242357.3056	6084
104	c0004s0019t01.nii.gz	3327	2457.285714	2787.742063	438.6666667	50.16666667	268.752381	242549.6327	0
105	c0004s0020t01.nii.gz	2372.714286	1405.294118	1843.741041	539.7493606	3.205494608	94.23902037	935748.24	0
106	c0004s0021t01.nii.gz	1746.357143	1385.526316	1492.918536	245.3571429	9.046296296	85.45507287	294306.332	0
107	c0004s0022t01.nii.gz	2861	2018.684829	2298.26346	215.125	0.263853391	49.46214224	270789.5037	0
108	c0004s0023t01.nii.gz	2136	1761.75	1988.083333	374.25	69.5	221.875	43473.33333	420.25
109	c0004s0024t01.nii.gz	3058.714286	2164.5	2619.215031	558.9285714	3.242134063	192.1128938	872563.5755	41412.25
110	c0004s0025t01.nii.gz	3170.090909	2053.518519	2353.051211	324.5721805	9.33622291	87.13056239	1052648.693	45660.90083
111	c0004s0026t01.nii.gz	1745.666667	1627	1686.333333	118.6666667	118.6666667	118.6666667	90000	29240.22222
112	c0004s0027t01.nii.gz	2650.666667	1733.44	2085.428841	917.2266667	90.16869565	439.2622222	205678.6464	53449.33333
113	c0004s0028t01.nii.gz	1838	1456.5	1628.513853	258.3571429	40.16666667	159.9642857	33440.4167	0
114	c0004s0029t01.nii.gz	3096.666667	1320.87234	2128.998786	547.8188259	1.013670257	103.0375717	594304.6836	9430.222222
115	c0004s0030t01.nii.gz	1488	1079.176471	1247.835784	408.8235294	199.1666667	280.1601307	159876.263	46440.25
116	c0004s0031t01.nii.gz	2082.481781	1466.862069	1786.109857	296.2222222	2.762626643	48.99302592	623116.9591	122270
117	c0004s0032t01.nii.gz	1954.411765	1574.659574	1765.53028	127.3829787	0.825383772	49.8070659	294283.86	38848.88889
118	c0004s0033t01.nii.gz	1936	1322.125	1597.451923	613.875	212.1057692	412.9903846	279997.4844	0
119	c0004s0034t01.nii.gz	2554.5	1195.822222	1812.441895	483.0172414	4.064102564	132.3814553	711987.9247	25863.1875
120	c0005s0003t01.nii.gz	192.8333333	112.7648903	138.5395592	21.21044304	0.317817723	6.675835872	1330.089403	42.47222222

	file	Max Intensity	Min Intensity	Average Intensity	Max Δ Intensity	Min Δ Intensity	Average Δ Intensity	Max Variance	Min Variance
121	c0005s0006t01.nii.gz	236	111	168.3136573	40.87100737	2.166666667	15.13287526	7914.305556	282.5
122	c0005s0007t01.nii.gz	282.3333333	101.8176217	151.1706634	26.97452137	0.005703212	4.559153761	2464.543816	103.3365042
123	c0005s0008t01.nii.gz	222.7777778	155.7894737	193.0123987	15.71052632	0.06779661	5.275134202	4258.975102	119.5061728
124	c0005s0009t01.nii.gz	258.0434783	194.7457627	226.9056516	21.04347826	0.025315315	3.737081598	3423.537231	150
125	c0005s0010t01.nii.gz	300.6	161.2857143	214.0431377	70.6	2.363636364	26.16948052	5774.237654	169
126	c0005s0011t01.nii.gz	223.2142857	147.225	185.6905938	39.00874126	0.935483871	11.80775789	3854.301769	212.9166667
127	c0005s0012t01.nii.gz	140.4090909	96.88	118.7748822	21.125	0.486522316	8.654828759	2889.810727	42.25
128	c0005s0013t01.nii.gz	164.4444444	48.79927007	90.19570417	60.73846154	0.004251624	3.772870692	3934.898859	325.76
129	c0005s0014t01.nii.gz	236.75	171.8571429	205.7691937	32.95454545	0.238181818	6.71004329	2246.798476	93.08333333
130	c0005s0017t01.nii.gz	260.6666667	183.1825095	215.7924915	22.60952381	0.033279545	3.828470208	3496.954057	53.55555556
131	c0005s0018t01.nii.gz	277.7019231	244	260.5015895	13.28110646	0.01875476	5.632790274	1561.752975	0
132	c0005s0021t01.nii.gz	235.1111111	153.825	190.1593076	61.77777778	1.955665025	31.16453886	1827.194375	163.6326531
133	c0005s0024t01.nii.gz	264.2	256.0769231	260.9709402	6.58974359	0.866666667	3.894871795	105.147929	60.56
134	c0005s0026t01.nii.gz	154.75	131	140.25	23.75	19.75	21.75	2298.6875	35.5
135	c0005s0027t01.nii.gz	196	65	158.7922183	65.75	3.641176471	23.63656863	1432.020833	0
136	c0005s0028t01.nii.gz	221	67	157.9307071	74	3.616071429	27.20634921	2223.718112	0
137	c0005s0029t01.nii.gz	121.6666667	104.3333333	113	17.33333333	17.33333333	17.33333333	1246.888889	470.8888889
138	c0005s0030t01.nii.gz	135.7009848	40.66666667	96.41603734	46.1875	0.042559899	4.94448738	5407.200527	180.2222222
139	c0005s0031t01.nii.gz	288	232.7966102	256.7435012	23	0.591666667	13.01959746	1457.348463	0
140	c0005s0035t01.nii.gz	252.525	183.5169082	219.6965009	29.64285714	0.022491039	5.771549122	4303.222595	25
141	c0005s0036t01.nii.gz	301.1052632	215.6964286	248.3701428	22.81637427	2.399192132	8.621231108	2520.764987	257.8836565
142	c0005s0040t01.nii.gz	285.375	250.625	268.1666667	34.75	17.875	26.3125	969.984375	252.75
143	c0005s0042t01.nii.gz	277.3684211	153.5227273	187.8800945	43.05641026	0.329059829	8.874535266	6010.866151	136.9695291
144	c0005s0043t01.nii.gz	183.45	118.8235294	152.8259129	24.12903226	0.369565217	7.713867135	1846.086505	0.25
145	c0005s0044t01.nii.gz	151.5	91.5	113.5	60	22	39	1206.583333	167.25
146	c0005s0045t01.nii.gz	392.1666667	231.0841121	281.0511686	96.38888889	9.340760389	32.54051892	7682.088521	1379.138889
147	c0005s0047t01.nii.gz	303.5185185	196.875	269.9809924	53.725	3.518518519	18.9720679	3011.141274	195.4736842
148	c0005s0048t01.nii.gz	306	199.125	229.1602727	106.875	6.603636364	36.93931818	2330.859375	0
149	c0005s0049t01.nii.gz	215	153.6666667	183.747807	61.33333333	7.49122807	37.61111111	4240.975069	934.8571429

	Average Variance	Max Delta Variance	Min Delta Variance	Average Delta Variance	Avg Delta/Avg Intensity
0	157.5194358	100.6811003	1.573736995	34.52282003	9.16%
1	72.52349206	44.38861426	0.989436445	14.63063017	2.32%
2	92.88574791	34.83373084	1.996294611	12.99563099	7.08%
3	72.96656981	41.00382308	0.969095399	11.59171128	5.42%
4	60.93158556	41.01880118	25.8016	31.29007649	20.57%
5	65.48195192	61.11049971	0.028055763	10.00584061	4.18%
6	90.03655388	64.49704619	0.564776602	14.1320881	2.51%
7	42.26578885	27.58052454	1.76705493	8.855896685	1.64%
8	65.61312001	82.08602444	0.341198152	16.02396444	2.05%
9	79.31809786	102.9183673	3.365672904	26.02172958	4.38%
10	91.31471855	156.5203728	1.2448721	34.53307418	4.09%
11	79.20257032	76.62288401	0.109683668	12.64317419	1.82%
12	76.43632759	58.5783987	0.185904709	15.87544706	2.39%
13	93.37280614	89.70343316	0.302915087	8.375300285	4.89%
14	81.06701856	97.44801116	0.343508349	15.11062186	4.25%
15	41.95471583	128.0292586	0.004616062	6.495130377	3.62%
16	100.7493702	145.2461533	0.845974841	31.10650354	7.99%
17	137.4981481	79.31888889	75.573333333	77.44611111	4.30%
18	87.23889365	103.7018503	0.302700512	20.20908913	4.45%
19	103.5997577	114.0274511	4.747324825	72.09059644	15.83%
20	123.475677	88.56857671	8.091109082	41.69900625	8.68%
21	131.0416223	165.2399376	0.276985195	27.32655854	5.19%
22	90.92446606	70.58343927	0.207213448	8.947384182	2.81%
23	129.5143811	108.6005716	4.921103956	63.9791922	14.35%
24	152.2140262	74.24339313	0.45240799	25.36618786	8.04%
25	93.54968981	106.7953469	2.762345679	37.79900283	8.73%
26	45.85516593	43.43299121	32.10474025	39.85462789	11.61%
27	77.28554041	52.33649438	12.72986354	35.70657725	9.65%
28	29.13021418	41.06417872	14.5	25.64164371	6.06%
29	52.62747275	76.05614604	4.246621423	44.56836286	4.29%
30	63.33767825	136.8333333	1.798888889	32.64631114	6.22%
31	155681.7195	126420.1251	24553.42292	80343.33598	12.54%
32	42261.64925	61497.29386	118.0049469	26992.00948	4.89%
33	308669.1216	240319.0208	38630.5186	111826.2962	7.87%
34	194871.8869	238092.9245	429.6944444	78997.30263	6.62%
35	212918.7733	162408.7333	3687.552827	48641.56888	5.24%
36	90896.58102	48097.52083	26547.29861	37322.40972	1.02%
37	181676.4864	159065.9025	1310.998724	69925.19625	5.20%
38	63845.97262	117394.8084	1136.005625	58803.08333	8.53%
39	124864.9808	258425.56	17309.73891	109624.4434	8.71%
40	96074.01103	104032.598	893.828247	21484.24886	3.68%

	Average Variance	Max Delta Variance	Min Delta Variance	Average Delta Variance	Avg Delta/Avg Intensity
41	69639.2105	59859.67675	27.15292517	27194.42524	2.78%
42	31364.04418	20880.31768	2749.08642	13665.82446	3.27%
43	76046.12954	56497.77363	1263.017483	30516.11546	4.06%
44	341603.1743	322611.2343	27589.03581	133791.8257	10.15%
45	128215.1286	139763.099	49441.51562	79931.95929	10.09%
46	225698.8887	256191.4097	26981.79237	133568.2027	11.87%
47	47653.93132	59218.3288	2793.532313	35915.23611	6.67%
48	174997.0773	254941.7778	4172.261517	77954.71777	7.13%
49	189259.592	201657.9191	1768.799965	57424.03677	3.08%
50	261304.5032	241085.4318	4760.578692	76239.67955	5.38%
51	135130.2958	123170.0556	5118.755669	61509.30261	7.34%
52	170683.3629	284890.6939	34012.88388	124938.4772	16.58%
53	213976.6808	258346.8827	0	91009.60725	10.42%
54	105539.5328	134406.912	2493.327903	53318.24053	3.65%
55	68889.58598	131182.6316	5828.114912	54217.38551	4.98%
56	248434.2561	188732.7282	2225.386931	83436.42757	7.31%
57	89536.16647	276542.0828	8598.991736	135967.0414	11.89%
58	136820.3487	145748.082	52707.26315	112281.8601	31.57%
59	171387.1484	123296.4297	709.283179	52847.25865	4.64%
60	48008.60871	42759.73254	6600.815093	23035.81658	2.49%
61	31234.33928	45718.64909	7.5625	17158.50058	4.97%
62	29566.11806	54769.6875	20841.02083	37805.35417	23.28%
63	78553.39847	88187.08297	11099.42293	37297.94621	13.42%
64	27254.28496	29110.51474	0	5330.145138	4.84%
65	87991.72084	96773.17263	1757.268781	34120.81444	4.54%
66	129783.1642	98714.73061	153.3988954	22203.42775	2.45%
67	103081.8978	84224.3542	6469.245018	23454.57104	9.89%
68	49475.38327	66894.69953	9209.656443	31234.67998	5.94%
69	71221.66027	50567.423	9539.655527	30053.53927	18.96%
70	111035.4239	62759.26553	12646.31124	41055.06064	6.70%
71	56287.02714	89857.06255	9240.585589	32653.48061	6.98%
72	87955.41022	71374.80061	2583.402622	22480.95044	11.90%
73	48997.05603	34602.63767	25719.58757	29186.67434	9.32%
74	40536.48393	40428.9514	1794.153015	15451.07093	5.70%
75	82127.05793	157559.6468	525.05106	32966.77745	5.11%
76	66996.46385	60256.85938	4403.291236	20879.44771	5.28%
77	54526.26599	77860.09	9522.294661	41353.06063	21.96%
78	26657.04316	66869.22917	1664.359375	27307.71616	5.07%
79	46607.53454	52586.40207	6369.762066	29912.91393	18.97%
80	37930.42133	48630.14782	4.779356388	17653.71098	6.69%

	Average Variance	Max Delta Variance	Min Delta Variance	Average Delta Variance	Avg Delta/Avg Intensity
81	75932.86845	120084.8594	3844.965624	38411.37689	6.42%
82	18736.61758	38909.53215	12967.15563	23001.95867	8.28%
83	76722.04793	70264.69388	877.8010204	27391.13014	4.30%
84	25922.79802	31585.82094	10350.54424	17158.44751	8.96%
85	76729.09116	80721.33506	2325.961349	29768.55956	7.01%
86	43089.75625	92055	2809	30580.85977	22.10%
87	233465.3225	255645.9462	121490.979	195513.605	13.73%
88	174905.1148	265013.7843	13225.58202	105826.1325	14.94%
89	475276.1783	378469.9335	668.3690024	45120.55993	3.59%
90	236343.4392	110434.8232	880.6974555	31664.37294	1.80%
91	344814.5082	278544.1912	7451.413348	72669.13038	4.86%
92	108568.7509	120390.1924	9084.282727	45413.29558	6.99%
93	316930.0803	715175.5663	7279.588551	202422.3795	3.73%
94	343458.5667	281906.5034	7980.390123	143556.2756	7.82%
95	638584.1996	335838.3806	762.4473196	61732.59037	2.48%
96	102569.5427	136459.6389	14208.36111	80810.01505	5.45%
97	45609.25	91218.5	91218.5	91218.5	33.90%
98	612810.9998	286714.9993	1276.884152	78625.67741	8.42%
99	232858.8055	210597.408	117.5357672	49133.71805	2.35%
100	231339.94	265854.61	96598.59988	181226.6049	16.61%
101	299567.4495	123332.25	2786.497041	54493.99461	8.01%
102	161534.4713	65259.76914	467.8352741	27098.88099	2.64%
103	163488.8822	121969.8056	3268.961736	63261.62594	11.77%
104	102216.1656	198728.5556	93439.22222	145079.442	9.64%
105	319480.5994	671667.284	548.5457093	120796.6443	5.11%
106	186444.2495	214019.1111	19742.8618	92944.98612	5.72%
107	158948.3153	97675.73438	85.20050187	19770.21841	2.15%
108	23270.42361	43053.08333	17555.64583	30304.36458	11.16%
109	434115.5596	702853.2806	4240.186091	220536.6856	7.33%
110	588665.2349	239468.8186	1849.455321	76430.7878	3.70%
111	59620.11111	60759.77778	60759.77778	60759.77778	7.04%
112	134454.7356	152229.3131	26904.29616	77338.20871	21.06%
113	220801.7174	303313.5207	894.4348944	125958.5349	9.82%
114	198123.8122	275586.1135	375.8729923	50627.85909	4.84%
115	98615.17547	102531.463	29076.87409	71989.15865	22.45%
116	394758.3975	114780.9982	232.5766548	35939.21697	2.74%
117	146330.9191	143416.2959	3015.780544	38292.62779	2.82%
118	119917.8873	279997.4844	200241.3069	240119.3956	25.85%
119	437432.6228	288550.7185	1704.595513	87837.65232	7.30%
120	771.0308944	382.1803091	5.178767141	118.2355114	4.82%

	Average Variance	Max Delta Variance	Min Delta Variance	Average Delta Variance	Avg Delta/Avg Intensity
121	3905.664207	7264.805556	53.7588772	1625.603708	8.99%
122	1338.421716	985.8439158	3.676135368	161.7787053	3.02%
123	1614.550576	1108.112968	2.860172291	380.9101346	2.73%
124	1782.174771	847.1771656	11.6372245	175.7409733	1.65%
125	3064.541798	3458.605001	303.6875	1601.647084	12.23%
126	1686.129664	1782.391369	175.2891581	827.1273464	6.36%
127	1983.179742	1806.109375	1.4891359	432.9172404	7.29%
128	1974.438886	675.125846	0.855955798	158.9134334	4.18%
129	981.4193282	1052.456572	8.667382704	259.7530416	3.26%
130	1463.923828	680.6645967	2.5	159.6275588	1.77%
131	640.3461806	665.1174531	2.144609445	216.5731827	2.16%
132	850.806073	905.8608071	757.7009148	818.3587773	16.39%
133	85.82667222	38.16222222	6.425706772	27.20235956	1.49%
134	974.2847222	2263.1875	1710.020833	1986.604167	15.51%
135	497.2306347	942.299759	42.64756944	386.4610683	14.89%
136	788.3558244	1102.924461	0	493.1595805	17.23%
137	858.8888889	776	776	776	15.34%
138	2403.141684	2423.011719	2.242014996	274.6873608	5.13%
139	471.8749164	726.456536	102.8271528	376.387654	5.07%
140	1640.69755	1203.335058	3.907063033	329.6408996	2.63%
141	1506.577211	850.9522164	20.57059275	382.6914062	3.47%
142	607.9895833	717.234375	368.75	542.9921875	9.81%
143	3483.883749	2259.2081	19.4128289	532.7830304	4.72%
144	575.3312991	862.5707711	4.194717954	186.4743559	5.05%
145	531.7083333	1039.333333	345.5	783.7222222	34.36%
146	4511.057684	3276.811728	325.9699448	1491.914439	11.58%
147	1367.593143	2186.669375	26.07272377	487.8312994	7.03%
148	992.9724542	2330.859375	611.5619041	1103.889688	16.12%
149	2707.576109	2869.809524	436.3084026	1899.095813	20.47%
			Average	8.27%	
			Variance	0.41%	

References

- [1] A.-R. Mansouri, *Mthe 493 projects 2020-2021 - b2 region tracking in an image sequence*.
- [2] M. C. Staff. "MRI," [Online]. Available at: <https://www.mayoclinic.org/tests-procedures/mri/about/pac-20384768>.
- [3] A. Berger. "Magnetic resonance imaging," [Online]. Available at: <https://www.ncbi.nlm.nih.gov/pmc/articles/PMC1121941/>.
- [4] F. Gaillard and A. Murphy. "MRI sequences (overview) — radiology reference article — radiopaedia.org," Radiopaedia, [Online]. Available at: <https://radiopaedia.org/articles/mri-sequences-overview> Last accessed: Oct. 17, 2020.
- [5] P. Jansen. "Concept: A project log for low-field mri," [Online]. Available at: <https://hackaday.io/project/5030-low-field-mri/log/15914-concept>.
- [6] In collab. with M. Biernacka, Feb. 18, 2021.
- [7] C. Verry, L. Sancey, S. Dufort, G. Le Duc, C. Mendoza, F. Lux, S. Grand, J. Arnaud, J.-L. Quesada, J. Villa, O. Tillement, and J. Balosso, "Treatment of multiple brain metastases using gadolinium nanoparticles and radiotherapy: Nano-rad, a phase i study protocol," *BMJ Open*, vol. 9, e023591, Feb. 2019.
- [8] "Brain lesions causes," Mayo Clinic, [Online]. Available at: <https://www.mayoclinic.org/symptoms/brain-lesions/basics/definition/sym-20050692> Last accessed: Apr. 8, 2021.
- [9] Frederik Barkhof, R. Smithuis, and M. Hazewinkel. "Multiple sclerosis," Radiology Assistant, [Online]. Available at: <https://radiologyassistant.nl/neuroradiology/multiple-sclerosis/diagnosis-and-differential-diagnosis>.
- [10] A.-R. Mansouri, *2020-2021 weekly mthe 493 tutorials*.
- [11] MIT-OpenCourseWare, *Discretizing odes : The forward euler method*. [Online]. Available at: <https://ocw.mit.edu/courses/aeronautics-and-astronautics/16-90-computational-methods-in-aerospace-engineering-spring-2014/numerical-integration-of-ordinary-differential-equations/discretizing-odes/1690r-the-forward-euler-method/>.
- [12] K. L. Ito, H. Kim, and S.-L. Liew, "A comparison of automated lesion segmentation approaches for chronic stroke t1-weighted MRI data," *bioRxiv*, 2018, Publisher: Cold Spring Harbor Laboratory _eprint: <https://www.biorxiv.org/content/early/2018/10/11/441451.full.pdf>. [Online]. Available at: <https://www.biorxiv.org/content/early/2018/10/11/441451>.
- [13] S.-L. Liew, J. M. Anglin, N. W. Banks, M. Sondag, K. L. Ito, H. Kim, J. Chan, J. Ito, C. Jung, N. Khoshab, S. Lefebvre, W. Nakamura, D. Saldana, A. Schmiesing, C. Tran, D. Vo, T. Ard, P. Heydari, B. Kim, L. Aziz-Zadeh, S. C. Cramer, J. Liu, S. Soekadar, J.-E. Nordvik, L. T. Westlye, J. Wang, C. Winstein, C. Yu, L. Ai, B. Koo, R. C. Craddock, M. Milham, M. Lakich, A. Pienta, and A. Stroud, "A large, open source dataset of stroke anatomical brain images and manual lesion segmentations," *Scientific Data*, vol. 5, no. 1, p. 180011, Feb. 20, 2018, Number: 1 Publisher: Nature Publishing Group. [Online]. Available at: <https://www.nature.com/articles/sdata201811> Last accessed: Oct. 17, 2020.
- [14] "Everything radiology departments need to consider before purchasing AI," [Online]. Available at: <https://www.healthimaging.com/topics/ai-emerging-technologies/radiology-consider-purchasing-ai> Last accessed: Apr. 10, 2021.
- [15] K. H. Zou, S. K. Warfield, A. Bharatha, C. M. Tempany, M. R. Kaus, S. J. Haker, W. M. Wells, F. A. Jolesz, and R. Kikinis, "Statistical validation of image segmentation quality based on a spatial overlap index," *Academic radiology*, vol. 11, no. 2, pp. 178–189, Feb. 2004. [Online]. Available at: <https://www.ncbi.nlm.nih.gov/pmc/articles/PMC1415224/> Last accessed: Apr. 10, 2021.
- [16] E. Morrin, *Biomedical image processing histogram equalization*. [Online]. Available at: <https://onq.queensu.ca/d2l/le/content/481626/viewContent/3035604/View>.
- [17] Y. -S. Chao, A. Sinclair, A. Morrison, D. Hafizi, and L. Pyke, "Canadian medical imaging inventory, 2019–2020," *Canadian Journal of Health Technologies*, vol. 1, no. 1, Jan. 29, 2021. [Online]. Available at: <https://canjhealthtechnol.ca/index.php/cjht/article/view/1510> Last accessed: Apr. 10, 2021.

- [19] N. W. John, “Segmentation of radiological images,” in *Image Processing in Radiology: Current Applications*, ser. Medical Radiology, E. Neri, D. Caramella, and C. Bartolozzi, Eds., Berlin, Heidelberg: Springer, 2008, pp. 45–54. [Online]. Available at: https://doi.org/10.1007/978-3-540-49830-8_4 Last accessed: Apr. 10, 2021.
- [20] R. A. Morey, C. M. Petty, Y. Xu, J. P. Hayes, H. R. Wagner, D. V. Lewis, K. S. LaBar, M. Styner, and G. McCarthy, “A comparison of automated segmentation and manual tracing for quantifying hippocampal and amygdala volumes,” *NeuroImage*, vol. 45, no. 3, pp. 855–866, Apr. 15, 2009. [Online]. Available at: <https://www.ncbi.nlm.nih.gov/pmc/articles/PMC2714773/> Last accessed: Apr. 10, 2021.
- [21] “Standalone medical device software harmonization (SaMD),” [Online]. Available at: <http://www.imdrf.org/workitems/wi-samd.asp> Last accessed: Apr. 10, 2021.
- [22] H. Canada. (Jun. 18, 2020). “Guidance document: Software as a medical device (SaMD): Definition and classification,” aem. Last Modified: 2020-06-18, [Online]. Available at: <https://www.canada.ca/en/health-canada/services/drugs-health-products/medical-devices/application-information/guidance-documents/software-medical-device-guidance-document.html> Last accessed: Apr. 10, 2021.
- [23] “Canadian association of medical radiation technologists — member code of ethics and professional conduct,” [Online]. Available at: <https://www.camrt.ca/mrt-profession/professional-resources/code-of-ethics/> Last accessed: Apr. 9, 2021.
- [24] “Code of ethics — national society of professional engineers,” [Online]. Available at: <https://www.nspe.org/resources/ethics/code-ethics> Last accessed: Apr. 9, 2021.
- [25] J. R. Geis, A. P. Brady, C. C. Wu, J. Spencer, E. Ranschaert, J. L. Jaremko, S. G. Langer, A. Borondy Kitts, J. Birch, W. F. Shields, R. van den Hoven van Genderen, E. Kotter, J. Wawira Gichoya, T. S. Cook, M. B. Morgan, A. Tang, N. M. Safdar, and M. Kohli, “Ethics of artificial intelligence in radiology: Summary of the joint european and north american multisociety statement,” *Radiology*, vol. 293, no. 2, pp. 436–440, Oct. 1, 2019, Publisher: Radiological Society of North America. [Online]. Available at: <https://pubs.rsna.org.proxy.queensu.ca/doi/full/10.1148/radiol.2019191586> Last accessed: Apr. 9, 2021.
- [26] T. M. University. “Does MRI have an environmental impact?” [Online]. Available at: <https://phys.org/news/2020-05-mri-environmental-impact.html> Last accessed: Apr. 10, 2021.
- [27] “Power management statistics: Information technology - northwestern university,” [Online]. Available at: <https://www.it.northwestern.edu/hardware/eco/stats.html> Last accessed: Apr. 10, 2021.
- [28] C. H. Douglas and M. R. Douglas, “Patient-friendly hospital environments: Exploring the patients’ perspective,” *Health Expectations: An International Journal of Public Participation in Health Care and Health Policy*, vol. 7, no. 1, pp. 61–73, Mar. 2004.
- [29] “Radiologist salary in canada,” [Online]. Available at: <https://www.erieri.com/salary/job/radiologist/canada> Last accessed: Apr. 11, 2021.
- [30] “Canada electricity prices, september 2020,” GlobalPetrolPrices.com, [Online]. Available at: https://www.globalpetrolprices.com/Canada/electricity_prices/ Last accessed: Apr. 10, 2021.
- [31] “CourseDescription - free surfer wiki,” [Online]. Available at: <http://surfer.nmr.mgh.harvard.edu/fswiki/CourseDescription> Last accessed: Apr. 11, 2021.
- [32] “Medical image analysis software market report, 2020-2027,” [Online]. Available at: <https://www.grandviewresearch.com/industry-analysis/medical-image-analysis-software-market> Last accessed: Apr. 7, 2021.

- [33] “Software development hourly rate in canada — PayScale,” [Online]. Available at: https://www.payscale.com/research/CA/Industry=Software_Development/Hourly_Rate Last accessed: Apr. 11, 2021.
- [34] “Grants and funding for biotech, lifesciences & medical - EVAMAX,” EVAMAX Group, [Online]. Available at: <https://evamax.com/biotech-lifesciences-medical-technology/> Last accessed: Apr. 10, 2021.
- [35] N. S.
bibinitperiod E. R. C. o. C. Government of Canada. (Jun. 28, 2016). “NSERC – idea to innovation grants,” Natural Sciences and Engineering Research Council of Canada (NSERC). Last Modified: 2020-10-30, [Online]. Available at: http://www.nserc-crsng.gc.ca/Professors-Professeurs/RPP-PP/I2I-INNOV_eng.asp Last accessed: Apr. 10, 2021.
- [36] I. Government of Canada. “Patent fees.” Last Modified: 2021-02-01 Publisher: Innovation, Science and Economic Development Canada, [Online]. Available at: <https://www.ic.gc.ca/eic/site/cipointernet-internetopic.nsf/eng/wr00142.html> Last accessed: Apr. 10, 2021.